SURGICAL ANATOMY OF MICRONEUROSURGICAL SULCAL KEY POINTS

Guilherme C. Ribas, M.D.
Department of Surgery,
University of São Paulo
Medical School,
São Paulo, Brazil

Alexandre Yasuda, M.D.
Department of Surgery,
University of São Paulo
Medical School,
São Paulo, Brazil

Eduardo C. Ribas, M.S.
Department of Surgery,
University of São Paulo
Medical School,
São Paulo, Brazil

Koshiro Nishikuni, M.D.
Department of Surgery,
University of São Paulo
Medical School,
São Paulo, Brazil

Aldo J. Rodrigues, Jr., M.D.
Department of Surgery,
University of São Paulo
Medical School,
São Paulo, Brazil

Reprint requests:
Guilherme C. Ribas, M.D.,
Department of Surgery,
University of São Paulo
Medical School,
Rua Eduardo Monteiro, 567,
São Paulo 05614-120 Brazil.

Received, October 26, 2005.
Accepted, August 2, 2006.

OBJECTIVE: The brain sulci constitute the main microanatomic delimiting landmarks and surgical corridors of modern microneurosurgery. Because of the frequent difficulty in intraoperatively localizing and visually identifying the brain sulci with assurance, the main purpose of this study was to establish cortical/sulcal key points of primary microneurosurgical importance to provide a sulcal anatomic framework for the placement of craniotomies and to facilitate the main sulci intraoperative identification.

METHODS: The study was performed through the evaluation of 32 formalin-fixed cerebral hemispheres of 16 adult cadavers, which had been removed from the skulls after the introduction of plastic catheters through properly positioned burr holes necessary for the evaluation of cranial–cerebral relationships. Three-dimensional anatomic and surgical images are displayed to illustrate the use of sulcal key points.

RESULTS: The points studied were the anterior sylvian point, the inferior rolandic point, the intersection of the inferior frontal sulcus with the precentral sulcus, the intersection of the superior frontal sulcus with the precentral sulcus, the superior rolandic point, the intersection of the intraparietal sulcus with the postcentral sulcus, the superior point of the parieto-occipital sulcus, the euryon (the craniometric point that corresponds to the center of the parietal tuberosity), the posterior point of the superior temporal sulcus, and the opisthocranion, which corresponds to the most prominent point of the occipital bossa. These points presented regular neural and cranial–cerebral relationships and can be considered consistent microsurgical cortical key points.

CONCLUSION: These sulcal and gyral key points can be particularly useful for initial intraoperative sulci identification and dissection. Together, they compose a framework that can help in the understanding of hemispheric lesion localization, in the placement of supratentorial craniotomies, as landmarks for the transsulcal approaches to periventricular and intraventricular lesions, and in orienting the anatomic removal of gyral sectors that contain infiltrative tumors.

KEY WORDS: Brain mapping, Burr holes, Cerebral cortex, Craniotomy

Neurosurgery 59[ONS Suppl 4]:ONS-177–ONS-211, 2006 DOI: 10.1227/01.NEU.0000240682.28616.b2

Although the sulci and the gyri of the brain are easily identified, particularly in standard magnetic resonance images (25, 49, 50, 51), their accurate visual transoperative recognition is notoriously difficult because of their common anatomic variations and their arachnoid cerebrospinal fluid and vessel coverings. Therefore, the study of the anatomy of particular sulcal key points that could serve as starting sites of sulcal identification and microsurgical dissection might be of some help.

The essential microsurgical sulcal and gyral key points to be studied are those constituted by the main sulci extremities and/or intersections and by the cortical sites that underlie particularly prominent cranial points. For practical purposes, these key points should be evaluated regarding their anatomic constancies and their neural and cranial–cerebral relationships.

The development of transcisternal, transfissural, and transsulcal approaches (32, 60, 95–97, 99, 101) established the sulci as fundamental anatomic landmarks of the brain. Particularly regarding the sulci and gyri relationships with the cranial vault, it is surprising that despite the huge knowledge of intracranial microanatomy developed during the

last three decades of the microneurosurgical era (54, 64, 75, 94–96, 101), little has been studied and published about anatomic cranial–cerebral correlations (22, 64, 65, 86). The cranial landmarks pertinent to the main cortical points used in neurosurgery are still based in the important contributions obtained in this field during the 19th century (3, 10–12, 42, 83, 84), which gave rise to modern neurosurgery by making these procedures more scientifically oriented and less exploratory (9, 30). In the present work, we attempted to study the previously described and new cranial–cerebral relationships in the light of more recent microanatomic knowledge.

The useful and practical intraoperative frameless imaging devices recently developed (90), besides being very expensive and not available in many centers, obviously should not substitute the anatomic tridimensional knowledge that every neurosurgeon should have to acquire and to continuously develop as part of his or her practice.

The aims of this study were 1) to establish the concept of sulcal key points and 2) to study their neural and cranial–cerebral relationships, mainly to ease the sulci intraoperative identification and to orient the placement of craniotomies.

MATERIALS AND METHODS

The present study was originally performed with 32 cerebral hemispheres from 16 adult cadavers at the Death Verification Institute of the Department of Pathology and at the Clinical Anatomy Discipline of the Department of Surgery of the University of São Paulo Medical School after authorization by the institution's Ethical Committee for Analysis of Research Projects.

The anatomic data obtained were pertinent to the evaluation of sulcal and cortical microneurosurgical key points that are listed in the Results section and that are presented in two parts. The first part covers characterization and neural relationships of topographically important sulcal points, and the second part covers cranial–cerebral relationships of topographically important sulcal points and prominent cranial points, which were studied with the aid of transcranial introduction of catheters.

After proper identification of the cadaver (*Table 1*) at the necropsy facilities regarding sex, age, race, weight, height, date, and necropsy number, and with the pathologist's consent, the study was carried out according to the steps outlined below.

1) Exposure of the cranial vault and accomplishment of the study procedures at the surgical suite of the Discipline of Clinical Anatomy of the Department of Surgery of the University of São Paulo Medical School. These procedures included A) exposure of the external cranial surface through a standard biauricular necroscopic incision and detachment of both temporal muscles, with a special concern for exposing the cranial sutures; B) accomplishment of 1.5-cm burr holes at the planned sites, as specified and listed in the Results section, with an electric drill (Dremel Moto-Tool; Dremel, Racine, WI); C) opening of the dura with a number 11 blade scalpel; and D) perpendicular introduction of plastic catheters (Plastic Tracheal Aspiration tubes, model Sonda-Suga number 08; Embramed, São Paulo, Brazil) approximately 7 cm in height and 2.5 mm in diameter with the aid of metallic guides.

TABLE 1. Characteristics of the studied cadavers (n = 16)

Sex	
Female	7 (44%)
Male	9 (56%)
Race	
Caucasian	10 (62.5%)
Black	6 (37.5%)
Age	
Range	36–85 yr
Average	62 yr
Weight	
Range	48–83 kg
Average	64 kg
Height	
Range	1.48–1.90 m
Average	1.67 m

2) Removal and storage of the specimen at the necropsy suite. These procedures included A) necroscopic circumferential opening of the skull and of the dura with proper saw and scissors by the necroscopic technical personnel under the pathologist's supervision; B) careful removal of the whole encephalon after basal divisions of the intracranial vessels and cranial nerves; C) evaluation of the internal aspects of the studied sites after opening the skull; D) replacement of the calvarium and closure of the scalp by the necropsy staff; E) evaluation of the proper positioning of the introduced catheters; and F) storage of the removed encephalons in 10% formalin solution with the specimen suspended by a string held at the basilar artery to prevent brain deformation.

3) Acquisition of the anatomic data at the clinical anatomy laboratory, including A) removal of a section of the brainstem at the midbrain level along with the cerebellum after adequate encephalon fixation for a least 2 months; B) removal of the arachnoidal membranes and the superficial vessels of the cerebral hemispheres with the aid of microsurgical loupes (Surgical Loupes of 3.5 enlargement; Designs for Vision, Inc., Ronkonkoma, NY) and/or surgical microscope (Zeiss Surgical Microscope, MDM model; Carl Zeiss Inc., Oberkochen, Germany); C) microscopic evaluation of the introduced catheters sites, as specified and listed in the Results section; D) separation of the cerebral hemispheres through the division of the corpus callosum, and evaluation of the catheter sites related to the ventricular cavities; and E) after the removal of the catheters, further microscopic evaluation of the sulci of interest for the study and their related key points, as specified and listed in the Results section.

The number of specimen evaluated regarding the sulci and the gyri observations was smaller than the initial sample be-

cause these data were obtained only in the cerebral hemispheres that had not been damaged during the analyses of cranial–cerebral relationships, which were performed when the brains were still harboring the catheters. The presentation of these results is thus reversed in position, for didactical purposes. The number of specimen of some of the analyzed data also differed because of eventual losses or incorrect positioning of a few catheters. The measurements were done in millimeters and always by the senior author (GCR), at least twice, and with the aid of millimetric bending plastic rulers and compasses.

For statistical analysis, all continuous variables were summarized by mean and standard deviation; because of the nonnormality of the data, range, median, and first and third quartiles were also included. Right and left sides were compared by Wilcoxon's matched-pairs signed ranks test (two tailed). A P value of less than 0.05 was taken as significant (77). For the statistical comparison of the right and left sides, only the paired specimen were considered. For this reason, the statistical findings pertinent to the total specimen, including the occasional nonpaired specimen, were not exactly related with the right and the left findings in these cases.

For the evaluation of the neural and cranial topographical relationships of the sulcal key points, the 90th percentile of the obtained values was calculated to permit a better estimation of the interval range of their distances through the analysis of the distribution of their positions. For the cases that presented opposite positionings, which were identified through positive and negative values, the 90th percentiles of both positive and negative groups were also distinctly calculated to permit a better descriptive analysis of their positioning distribution and range (48, 77). Finally, an interval range of up to 2 cm was considered acceptable for the surgical purposes of craniotomy placement and sulcal key points for intraoperative visual identification.

The stereoscopic illustrations displayed here were done with the anaglyphic technique as previously described by the senior author (GCR) (67). For their proper viewing, 1) use the reading glasses under the three-dimensional (3-D) red (left eye) and blue (right eye) glasses, 2) look at the anaglyphic images under good light conditions, and 3) leave the image about 30 cm away from your eyes and as flat as possible, focus at the deepest aspect of the image, and wait while adapting your 3-D view.

RESULTS

Characterization and Neural Relationships of Topographically Important Sulcal Points

The Anterior Sylvian Point: Identification, Location, and Morphology

The anterior sylvian point was identified in all cases and was located inferior to the triangular part and anterior/inferior to the opercular part of the inferior frontal gyrus (IFG) in all 18 specimen studied regarding this evaluation. The anterior sylvian point was characterized as an enlargement of the sylvian fissure caused by the usual retraction of the triangular part of the IFG in relation to the sylvian fissure, with a variable cisternal aspect: cisternal (3–4 mm), nine specimen (49%); wide cisternal (≥5 mm), five specimen (28%); small cisternal (2–3 mm), three specimen (17%); and poorly evident (≤2 mm), one specimen (6%).

The Central Sulcus and the Superior Rolandic Point

The central sulcus (CS) in this study was identified in all cases as a continuous sulcus not connected to any other sulci anteriorly or posteriorly; its superior extremity was situated inside the interhemispheric fissure (IHF) in all studied specimen. The intersection of the CS with the IHF superior margin, which evidently characterizes an important neurosurgical landmark and roughly corresponds to the CS superior extremity projection over the IHF superior margin, was studied here under its usual denomination of superior rolandic point (SRP) and was identified in each specimen.

The Inferior Rolandic Point

The CS inferior extremity, which was identified in all cases, was superior to the sylvian fissure in 25 specimen (83%) and was located inside the sylvian fissure in five (17%) out of the 30 specimen studied regarding this observation, with an average distance of 0.54 ± 0.62 cm superior to the sylvian fissure (*Table 2*).

The real intersection of the CS with the sylvian fissure, or the virtual CS and sylvian fissure intersection given by a CS prolongation, which corresponds to the CS inferior extremity projection over the sylvian fissure, was studied under the designation of inferior rolandic point (IRP).

The IRP was located at an average distance of 2.36 ± 0.50 cm posterior to the anterior sylvian point along the sylvian fissure (*Table 2*).

The Superior Frontal Sulcus and Its Posterior Extremity Point

The superior frontal sulcus (SFS) was parallel to the IHF in the 18 specimen evaluated regarding this verification and was completely continuous in nine (50%) of these specimen. The average length of its continuous posterior segment adjacent to the precentral sulcus was 5.74 ± 2.62 cm (*Table 2*).

The posterior extremity of the superior frontal sulcus (SFS) was found anterior to the precentral sulcus in one specimen (6%), coincident with the precentral sulcus in three specimen (17%) and posterior to the precentral sulcus in 14 specimen (77%), with an average distance of 0.69 ± 0.56 cm posterior to the precentral sulcus and 2.67 ± 0.37 cm lateral to the IHF (*Table 2*).

In the coronal plane, the SFS posterior extremity was related to the superior surface of the thalamus and, thus, the floor of the body of the lateral ventricle, in the 20 specimen that were evaluated regarding this relationship.

TABLE 2. Important sulcal points and related measurements[a]

	No.			Range	First quartile			Median		
	R	L	Total	Total	R	L	Total	R	L	Total
Distance CS inf extr–SyF	14	15	29	−1.00 to 1.20	0.50	0.45	0.50	0.50	0.70	0.60
Distance IRP–ASyP (along the SyF)	9	9	18	1.80 to 4.00	2.00	2.00	2.00	2.20	2.50	2.25
SFS posterior segment length	9	9	18	2.00 to 11.50	4.50	2.75	3.88	5.70	6.50	5.85
Distance SFS post extr–preCS	9	9	18	−0.50 to 1.50	0.40	0.00	0.23	0.60	0.80	0.80
Distance SFS post extr–IHF	9	9	18	2.00 to 3.30	2.35	2.45	2.48	2.90	2.50	2.55
IFS posterior segment length	9	9	18	1.00 to 6.20	2.75	1.40	1.95	3.70	2.30	3.25
Distance IFS post extr–preCS	9	9	18	−1.00 to 0.70	0.00	−0.50	−0.13	0.00	0.00	0.00
Distance IFS post extr–SyF	9	9	18	1.30 to 4.50	2.60	2.40	2.50	3.00	2.80	2.80
Distance IFS post extr–ASyP (parallel to the SyF)	9	9	18	0.00 to 2.30	0.90	0.60	0.78	1.00	0.80	0.90
IPS most evident segment length	9	9	18	1.30 to 5.00	1.63	2.13	2.00	3.60	2.75	3.20
Distance IPS ant extr–IHF	9	9	18	2.40 to 4.70	4.00	3.50	4.00	4.00	4.00	4.00
Distance IPS ant extr coronal plane–posterior aspect of splenium coronal plane	10	10	20	0.00 to 2.00	0.00	0.00	0.00	0.00	0.00	0.00
EOF length	9	9	18	1.40 to 3.50	1.50	1.90	1.65	2.00	2.50	2.00
Distance EOF/POS extr–postCS (along the IHF; precuneus anteroposterior length)	9	9	18	2.70 to 5.00	3.40	3.45	3.48	4.20	3.70	4.00

The Inferior Frontal Sulcus and Its Posterior Extremity Point

The inferior frontal sulcus (IFS) was parallel to the sylvian fissure in all 18 specimen, was found as a continuous sulcus in six specimen (33%), and was found as an interrupted sulcus in 12 specimen (67%). The average length of its continuous posterior segment adjacent to the precentral sulcus was 3.97 ± 1.37 cm in the right hemisphere and 2.83 ± 1.82 cm in the left hemisphere (*Table 2*).

The posterior extremity of the IFS was anterior to the precentral sulcus in four specimen (22%), coincident with the precentral sulcus in 10 specimen (56%), and posterior to the precentral sulcus in four specimen (22%), with average distances of 0.03 ± 0.48 cm anterior to the precentral sulcus, 2.84 ± 0.65 cm superior to the sylvian fissure, and 1.23 ± 0.48 cm from the anterior sylvian point along a parallel line to the sylvian fissure (distance of IFS posterior extremity vertical projection on the sylvian fissure from the anterior sylvian point) (*Table 2*).

The Intraparietal Sulcus and Its Anterior Extremity Point

The intraparietal sulcus (IPS) was parallel or almost parallel to the IHF in 16 specimen (89%), almost perpendicular to the IHF in two specimen (11%), continuous with the postcentral sulcus inferior portion in 15 specimen (83%), and noncontinuous with the postcentral sulcus in three specimen (17%). The most evident segment of the IPS was superior to only the supramarginal gyrus (SMG) in 10 specimen (56%) and superior to both the supramarginal and the angular gyri (AG) in eight specimen (44%), with an average length of 3.19 ± 1.17 cm (*Table 2*).

The IPS anterior extremity point, which corresponds to its most anterior point, was identified as a transition point between the IPS and the postcentral sulcus in 12 specimen (67%), as a distinct anterior extremity point of an IPS not continuous with the postcentral sulcus in two specimen (11%), and as not identifiable as a single distinct point in four specimen (22%) because of duplication and/or oblique or transverse morphology of the IPS. The IPS anterior extremity was situated at an average distance of 3.96 ± 0.67 cm lateral to the IHF (*Table 2*).

In the coronal plane, the IPS anterior extremity was posterior to the lateral ventricle atrium in all 20 specimen studied regarding this evaluation. It was at the level of the corpus callosum splenium in 15 specimen (75%) and posterior to this structure in five (25%) of these 20 specimen, with an average posterior distance of 0.23 ± 0.50 cm between the respective coronal planes (*Table 2*).

The IPS anterior extremity was related to the lateral ventricle atrium along a 30-degree posterior oblique plane in 19 specimen (95%), and required an inclination of 45 degrees to achieve this relationship in one specimen (5%).

The Superior Temporal Sulcus Posterior Portion and Its Posterior Extremity Point

The posterior point of the posterior segment of the superior temporal sulcus (postSTS) was defined in this study as the

TABLE 2. Continued

Third quartile			Mean			Standard deviation			Right × left (Wilcoxon; *P* value)	90th percentiles			Observations
R	L	Total	R	L	Total	R	L	Total		Total	Positive values	Negative values	
1.05	1.00	1.00	0.53	0.56	0.54	0.71	0.56	0.62	0.916	1.20	1.20	0.30	Negative, superior to SyF; positive, inferior to SyF
2.45	2.65	2.60	2.22	2.49	2.36	0.27	0.65	0.50	0.182				
6.50	8.50	6.88	5.59	5.89	5.74	1.94	3.28	2.62	0.866				
1.10	1.15	1.05	0.72	0.66	0.69	0.46	0.67	0.56	0.767	1.50	1.50	0.00	Negative, anterior to preCS; positive, posterior to preCS
3.20	2.80	2.93	2.78	2.56	2.67	0.42	0.29	0.37	0.122				
5.25	4.50	5.00	3.97	2.83	3.40	1.37	1.82	1.67	0.036*				Right- and left-side measurements significantly different ($P < 0.05$)
0.25	0.30	0.13	0.01	−0.08	−0.03	0.45	0.54	0.48	0.674	0.61	0.65	0.00	Negative, anterior to preCS; positive, posterior to preCS
3.45	2.95	3.10	3.10	2.58	2.84	0.67	0.55	0.65	0.075				
1.50	0.90	1.20	1.23	0.72	0.98	0.48	0.33	0.48	0.007*				Right- and left-side measurements significantly different ($P < 0.05$)
4.38	4.40	4.28	3.14	3.13	3.19	1.34	1.17	1.17	0.866				
4.50	4.50	4.50	4.00	3.92	3.96	0.61	0.75	0.67	0.684				
0.25	0.50	0.38	0.30	0.15	0.23	0.67	0.24	0.50	0.705				
2.75	2.80	2.80	2.10	2.36	2.23	0.75	0.47	0.62	0.204				
4.40	4.50	4.50	3.97	3.93	3.95	0.70	0.61	0.64	0.779				

[a] R, right; L, left; CS inf extr, central sulcus inferior extremity; SyF, sylvian fissure; IRP, inferior rolandic point; ASyP, anterior sylvian point; SFS, superior frontal sulcus; SFS post extr, superior frontal sulcus posterior extremity point; preCS, precentral sulcus; IHF, interhemispheric fissure; IFS, inferior frontal sulcus; IFS post extr, inferior frontal sulcus posterior extremity point; IPS ant extr, intraparietal sulcus anterior extremity; EOF, external occipital fissure; EOF/POS, EOF medial point that corresponds to the parieto-occipital sulcus' most superior point; postCS, postcentral sulcus. A *P* value of less than 0.05 is significant for right side measurements different than left side measurements. Measurements are in centimeters.

posterior extremity of its most clearly distal segment identified as a single sulcal trunk before the frequent superior temporal sulcus (STS) distal bifurcation. This clearly identifiable STS posterior segment was in continuity with the more anterior part of the STS in 23 specimen (88%), was identified as a single trunk posterior to a STS interruption in two specimen (8%), and was characterized as a local secondary sulcus in one (4%) out of the 26 specimen evaluated regarding this analysis.

The postSTS was systematically posterior and inferior to the posterior sylvian point in all 20 specimen studied regarding this evaluation, and the postSTS was related with the lateral ventricle atrium along a 45-degree posteriorly oblique plane in 18 specimen (90%), and along a 30- to 45-degree posteriorly oblique plane in two specimen (10%).

The External Occipital Fissure and Its Medial Extremity Point

The external occipital fissure (EOF) (9), which corresponds to the extension of the parieto-occipital sulcus (POS) along the superolateral face of the cerebral hemisphere, was evident and well defined in all 18 specimen evaluated for this verification, with an average length of 2.23 ± 0.62 cm (*Table 2*).

The EOF medial point (EOF/POS), which corresponds to the superior extremity of the POS on the IHF, was also identified in all of these 18 specimen and was situated at an average distance of 3.95 ± 0.64 cm posterior to the postcentral sulcus (*Table 2*), a distance that corresponds to the precuneus longitudinal length.

Cranial–Cerebral Relationships of the Topographically Important Sulcal Points and of Prominent Cranial Points

Anterior Sylvian Point

The relationships of the anterior sylvian point with the external cranial surface were evaluated through the study of the topographic correlations between the anterior sylvian point and a skull point that was designated as the anterior squamous point and defined as the central point of a 1.5-cm-diameter burr hole located on the most anterior segment of the squamous suture, superior to the sphenosquamous suture and just posterior to the sphenoparietal suture, and thus over the squamous suture just posterior to the H central bar that characterizes the pterion.

After its exposure, the pterion had an evident H morphology in 23 specimen (72%) and a nonsimilar H-shape in nine (28%) out of the 32 specimen evaluated, allowing an easy and proper anterior squamous point identification in all studied specimen.

TABLE 3. Important sulcal points and cranial-cerebral relationships and measurements[a]

	No.			Range	First quartile			Median		
	R	L	Total	Total	R	L	Total	R	L	Total
ASqP–ASyP vertical distance	13	13	27	−1.60 to 0.50	−0.30	−0.55	−0.50	0.00	0.00	0.00
ASqP–ASyP horizontal distance	13	13	27	−1.50 to 1.00	0.00	−0.25	0.00	0.00	0.00	0.00
SSaP–SRP distance	16	16	32	−1.50 to 1.20	−0.43	0.00	−0.15	0.00	0.00	0.00
SSqP–preAuDepr distance	15	15	30	3.50 to 5.00	3.50	3.50	3.50	4.00	4.00	4.00
SSqP–SyF distance	15	15	31[b]	−1.20 to 0.60	0.00	0.00	0.00	0.00	0.00	0.00
SSqP–IRP horizontal distance	15	15	31[b]	−2.40 to 1.80	−0.50	−0.60	−0.60	0.00	0.00	0.00
PCoP–SFS distance	16	16	32	−0.50 to 1.50	0.00	0.00	0.00	0.00	0.00	0.00
PCoP–preCS distance	16	16	32	−2.40 to 1.50	−1.20	−1.38	−1.28	−0.90	−0.95	−0.95
St–Br distance	11	11	22	7.00 to 9.00	7.00	7.00	7.00	8.00	7.50	7.90
St–IFS distance	15	15	30	−2.10 to 1.10	0.00	−0.50	−0.40	0.00	0.00	0.00
St–preCS distance	15	15	30	−2.00 to 0.80	−0.60	−0.70	−0.70	0.00	−0.30	−0.25
IPP–IPS distance	16	16	32	−0.50 to 2.00	0.00	0.00	0.00	0.40	0.15	0.30
IPP–postCS distance	16	16	32	0.00 to 2.50	0.50	1.00	0.83	1.55	1.30	1.35
TPP–postSTS distance	12	12	26[b]	−1.00 to 1.00	0.00	0.00	0.00	0.00	0.00	0.00
TPP–PSyP vertical distance	12	12	26[b]	0.00 to 2.40	1.00	1.30	1.00	1.40	1.50	1.50
TPP–PSyP horizontal distance	12	12	26[b]	1.00 to 4.00	2.13	1.28	1.50	2.50	1.50	1.80
TPP–PsyP direct distance	12	12	26[b]	1.00 to 4.20	2.50	1.50	1.75	2.55	2.00	2.40
La/Sa–EOF/POS distance	16	16	32	−0.50 to 1.20	0.00	0.00	0.00	0.35	0.00	0.00

Regarding the vertical position of the anterior sylvian point relative to the squamous suture, the anterior squamous point was superior to the anterior sylvian point in one specimen (4%), situated at the anterior sylvian point level in 19 specimen (70%), and inferior to the anterior sylvian point in seven (26%) out of the 27 specimen studied regarding this evaluation, with an average distance of 0.18 ± 0.41 cm inferior to the anterior sylvian point and without a significant difference between the right and the left sides (*Table 3*). Regarding the horizontal position of the anterior sylvian point along the squamous suture, the anterior squamous point was anterior to the anterior sylvian point in six specimen (22%), at the same level of the anterior sylvian point along the sylvian fissure in 15 specimen (56%), and posterior to the anterior sylvian point in another six (22%) out of the 27 specimen evaluated, with an average distance of 0.02 ± 0.53 cm anterior to the anterior sylvian point and without a significant difference between the two sides (*Table 3*). The 90th percentile values pertinent to the vertical positioning of the anterior squamous point relative to the anterior sylvian point (total, 0.00 cm; superior values, 0.00 cm; inferior values, 0.00 cm) and the 90th percentile values pertinent to the horizontal positioning of the anterior squamous point, relative to the anterior sylvian point (total, 0.68 cm; anterior, 0.00 cm; posterior, 0.92 cm) indicate a very close relationship between the anterior sylvian point and the most anterior segment of the squamous suture (*Table 3*).

Superior Rolandic Point

The superior rolandic point position relative to the external cranial surface was studied regarding its position relative to the central point of a 1.5-cm burr hole that was centered 5 cm posterior to the bregma and just lateral to the sagittal suture, and that was named the superior sagittal point. The bregma was located at an average distance of 12.69 ± 0.70 cm posterior to the nasion (*Table 4*).

TABLE 3. Continued

Third quartile			Mean			Standard deviation			Right × left (Wilcoxon; *P* value)	90th percentiles			Observations
R	L	Total	R	L	Total	R	L	Total		Total	Positive values	Negative values	
0.00	0.00	0.00	−0.15	−0.23	−0.18	0.28	0.53	0.41	0.416	0.00	0.00	0.00	Negative, inferior; positive, superior
0.25	0.15	0.00	0.09	−0.08	−0.02	0.38	0.64	0.53	0.463	0.68	0.92	0.00	Negative, anterior; positive, posterior
0.50	0.50	0.50	−0.03	0.23	0.10	0.67	0.48	0.59	0.099	0.94	1.10	0.00	Negative, anterior; positive, posterior
4.50	4.00	4.13	4.05	3.99	4.02	0.50	0.50	0.49	0.414				
0.00	0.30	0.00	−0.13	−0.03	−0.08	0.37	0.46	0.41	0.429	0.46	0.50	0.00	Negative, inferior; positive, superior
0.70	0.50	0.60	0.15	−0.13	−0.06	0.93	0.97	1.01	0.381	1.16	1.44	0.00	Negative, anterior; positive, posterior
0.00	0.00	0.00	0.02	0.13	0.07	0.14	0.43	0.32	0.462	0.44	0.48	0.00	Negative, lateral; positive, medial
−0.13	0.00	0.00	−0.87	−0.65	−0.76	0.71	0.88	0.79	0.401	0.00	1.38	0.00	Negative, anterior; positive, posterior
8.50	8.50	8.50	7.95	7.71	7.83	0.76	0.71	0.73	0.287				
0.00	0.00	0.00	−0.16	−0.17	−0.17	0.68	0.26	0.50	0.552	0.00	0.00	0.00	Negative, inferior; positive, superior
0.50	0.00	0.00	−0.26	−0.42	−0.34	0.82	0.61	0.71	0.266	0.68	0.75	0.00	Negative, anterior; positive, posterior
0.95	0.78	0.80	0.46	0.38	0.42	0.45	0.59	0.52	0.528	1.00	1.00	0.00	Negative, lateral; positive, medial
1.98	1.50	1.80	1.30	1.31	1.31	0.83	0.49	0.67	1.000	2.28			IPP always posterior to postCS
0.00	0.00	0.00	−0.03	0.00	−0.01	0.35	0.43	0.37	0.892	0.24	0.48	0.00	Negative, inferior; positive, superior
2.00	1.78	1.85	1.40	1.35	1.37	0.65	0.67	0.63	0.635				TPP always inferior to PSyP
3.08	1.68	2.50	2.54	1.55	2.00	0.85	0.43	0.82	0.008[c]				TPP always posterior to PSyP
3.50	2.40	2.65	2.80	1.98	2.35	0.91	0.46	0.80	0.012[c]				
0.50	0.23	0.50	0.34	0.13	0.23	0.39	0.37	0.39	0.059	0.94	0.98	0.00	Negative, anterior; positive, posterior

[a] R, right; L, left; ASqP, anterior squamous point; ASyP, anterior sylvian point; SSaP, superior sagittal point; SRP, superior rolandic point; SSqP, superior squamous point; preAuDepr, preauricular depression; SyF, sylvian fissure; IRP, inferior rolandic point; PCoP, posterior coronal point; SFS, superior frontal sulcus; preCS: precentral sulcus; St, stephanion (coronal suture and superior temporal line meeting point); Br, bregma; IFS, inferior frontal sulcus; IPP, intraparietal point; IPS, intraparietal sulcus; postCS, postcentral sulcus; TPP, temporoparietal point; PSyP, posterior sylvian point; La/Sa, lambdoid–sagital point; EOF/POS, external occipital fissure medial point, equivalent to the most superior point of the parieto-occipital sulcus. Measurements are in centimeters.

[b] Different total number attributable to inclusion of nonpaired specimen, as explained in the Patients and Methods section.

[c] Significant difference between right and left sides.

The superior sagittal point was anterior to the SRP in eight specimen (25%), at the SRP level in 12 specimen (37.5%), and posterior to the SRP in 12 (37.5%) of the 32 studied specimen, at an average distance of 0.10 ± 0.59 cm posterior to the SRP, without any significant differences between sides (*Table 3*). Its 90th percentile values (total, 0.94 cm; posterior values, 1.10 cm; anterior values, 0.00 cm) indicate a predominant posterior distribution of the superior sagittal point relative to the SRP (*Table 3*).

Inferior Rolandic Point

The inferior rolandic point, which corresponds to the CS inferior extremity projection on the sylvian fissure, was studied for its position relative to the external cranial surface regarding its position relative to the central point of a 1.5-cm burr hole located at the intersection of the squamous suture with a vertical line originating at the preauricular depression. This point was called the superior squamous point and was found, in all cases, to be situated along the most superior segment of the squamous suture. The height of the squamous suture at this level, which corresponds to the superior squamous point–preauricular depression distance, had an average value of 4.02 ± 0.49 cm, without significant differences between sides (*Table 3*).

The superior squamous point was found superior to the sylvian fissure in five specimen (16%), at the sylvian fissure

TABLE 4. Cranial midline measurements[a]

	No.	Range	First quartile	Median	Third quartile	Mean	Standard Deviation
Na-Br	16	12.00–14.00	12.00	12.50	13.00	12.69	0.70
Na-La	16	24.00–28.00	25.00	25.00	26.00	25.63	1.16
Br-La	16	12.00–14.00	12.50	13.00	13.13	12.94	0.68
La-OpCr	16	1.00–4.00	2.38	3.00	4.00	3.00	0.93

[a] Na, nasion; Br, bregma; La, lambda; OpCr, opisthocranion. Measurements are in centimeters.

level in 20 specimen (65%), and inferior to the sylvian fissure in six (19%) out of the 31 specimen evaluated regarding this analysis, with an average distance of 0.08 ± 0.41 cm inferior to the sylvian fissure and without significant differences between sides (*Table 3*). Relative to the IRP, the superior squamous point was anterior in 10 specimen (32%), at the same level in nine specimen (29%), and posterior in 12 specimen (39%), at an average distance of 0.06 ± 1.01 cm anterior to the IRP and without right and left significant differences (*Table 3*). The 90th percentile values of the superior squamous point vertical distance from the IRP (total, 0.46 cm; superior values, 0.50 cm; inferior values, 0.00 cm) and the horizontal distance from the IRP (total, 1.16 cm; posterior, 1.44 cm; anterior, 0.00 cm) indicate a very appropriate vertical correlation between the distribution of these two points, with a predominant posterior distribution of the superior squamous point position relative to the IRP (*Table 3*).

The Superior Frontal and Precentral Sulci Meeting Point

The real SFS and precentral sulcus meeting point, or virtual meeting point given by the intersection of the precentral sulcus with a posterior SFS prolongation (SFS/precentral sulcus), had its external cranial projection examined regarding its relationships with the central point of a 1.5-cm burr hole located 1 cm posterior to the coronal suture and 3 cm lateral to the sagittal suture. This point was called the posterior coronal point (PCoP).

Relative to the SFS, the PCoP was lateral to the SFS in two specimen (6%), coincident with the SFS in 26 specimen (81%), and medial to the SFS in four specimen (13%), at an average distance of 0.07 ± 0.32 cm medial to the SFS and without right and left significant differences (*Table 3*). Its 90th percentile values (total, 0.44 cm; medial values, 0.48 cm; lateral values, 0.00 cm) corroborate their close relationship (*Table 3*).

Relative to the precentral sulcus, the PCoP was anterior to the precentral sulcus in 22 specimen (69%), at the precentral sulcus level in eight specimen (25%), and posterior to the precentral sulcus in two specimen (6%), at an average distance of 0.76 ± 0.79 cm anterior to the precentral sulcus and without significant differences between sides (*Table 3*). Its 90th percentiles (total, 0.00 cm; posterior values, 1.38 cm; anterior values, 0.00 cm) indicate their close relationship (*Table 3*).

The Inferior Frontal and Precentral Sulcus Meeting Point

The real inferior frontal sulcus (IFS) and precentral sulcus meeting point, or virtual meeting point given by the intersection of the precentral sulcus with a posterior IFS prolongation (IFS/precentral sulcus), had its external cranial projection examined regarding its position relative to the central point of a 1.5-cm burr hole at the intersection of the coronal suture and the superior temporal line, a location that constitutes a craniometric point called the stephanion (St) (11, 59). The average distance from the St to the bregma along the coronal suture was 7.83 ± 0.73 cm, without right and left significant differences (*Table 3*).

Relative to the IFS, the St was superior to the IFS in one specimen (3%), at the IFS level in 21 specimen (70%), and inferior to the IFS in eight (27%) out of the 30 specimen studied regarding this evaluation, at an average distance of 0.17 ± 0.50 cm inferior to the IFS and without significant differences between sides (*Table 3*). Its 90th percentiles (total, 0.00 cm; superior values, 0.00 cm; inferior values, 0.00 cm) corroborate their very close relationship (*Table 3*).

Relative to the precentral sulcus, the St was anterior in 16 specimen (53%), at the same level in nine specimen (30%), and posterior in five specimen (17%), at an average distance of 0.34 ± 0.71 cm anterior to the precentral sulcus (*Table 3*). Its 90th percentiles (total, 0.68 cm; posterior values, 0.75 cm; anterior values, 0.00 cm) corroborate their close relationship (*Table 3*).

The Intraparietal and Postcentral Sulci Meeting Point

The intraparietal sulcus (IPS) and postcentral sulci transitional point or meeting point, given by a real intersection or by a postcentral sulcus intersection with an anterior IPS prolongation and designated here as an IPS and postcentral sulcus meeting point (IPS/postcentral sulcus), had its external cranial surface projection evaluated through the study of its relationships with the central point of a 1.5-cm burr hole centered 5 cm anterior to the λ and 4 cm lateral to the sagittal suture, referred to here as the intraparietal point (IPP). The λ was located at an average distance of 25.63 ± 1.16 cm posterior to the nasion and 12.94 ± 0.68 cm posterior to the bregma (*Table 4*).

The IPP was found lateral to the IPS in one specimen (3%), at the level of the IPS in 13 specimen (41%), and medial to the IPS in 18 (56%) of the 32 studied specimen, at an average distance of 0.42 ± 0.52 cm medial to the IPS (*Table 4*). Its 90th

percentiles (total, 1.00 cm; medial values, 1.00 cm; lateral values, 0.00 cm) indicate the predominant medial distribution of the IPP relative to the IPS (*Table 3*).

Relative to the postcentral sulcus, the IPP was found to be posterior to the postcentral sulcus in all specimen, at an average distance of 1.31 ± 0.67 cm *(Table 3*) and without significant differences between sides (*Table 3*). Its 90th percentiles (total, 2.28 cm) emphasize the predominant posterior distribution of the IPP relative to the postcentral sulcus (*Table 3*).

The Superior Temporal Sulcus Posterior Portion Point

The superior temporal sulcus posterior portion and posterior point (postSTS) external cranial projection was studied through its relationships with the central point of a 1.5-cm burr hole centered 3 cm vertically above the meeting point of the parietomastoid suture and the squamous suture, referred to here as the temporoparietal point, which was found to be just below the posterior aspect of the superior temporal line in all cases.

The temporoparietal point was superior to the postSTS in two specimen (8%), at the same level of the postSTS in 21 specimen (80%), and inferior to the postSTS in three (12%) out of the 26 specimen studied regarding this observation, at an average distance of 0.01 ± 0.37 cm inferior to the postSTS and without any significant differences between sides (*Table 3*). Its 90th percentiles (total, 0.24 cm; superior values, 0.48 cm; inferior values, 0.00 cm) corroborate their close relationship (*Table 3*).

The temporoparietal point position was also studied in relation to the posterior sylvian point and was found to be situated posterior and inferior to the posterior sylvian point in all cases. The temporoparietal point was, on average, 1.37 ± 0.63 cm inferior to the posterior sylvian point, without significant differences between sides, and 2.54 ± 0.85 cm posterior to the posterior sylvian point in the right side and 1.55 ± 0.43 cm posterior to the posterior sylvian point in the left side, with a significant difference between the two sides. The average direct distance from the posterior sylvian point was 2.80 ± 0.91 cm in the right side and 1.98 ± 0.46 cm in the left side, with a significant difference between sides (*Table 3*).

The External Occipital Fissure Medial Point

The external occipital fissure (EOF) medial point (EOF/POS), which is situated on the IHF and which corresponds to the most superior point of the parietoccipital sulcus (POS) when it reaches the IHF, had its external cranial projection studied through its relationships with the central point of a 1.5-cm burr hole located at the angle between the lambdoid and the sagittal sutures, referred to here as lambdoid/sagittal point (La/Sa).

The La/Sa was situated anterior to the EOF/POS in two specimen (6%), at the EOF/POS level in 16 specimen (50%), and posterior to the EOF/POS in 14 specimen (44%), at an average distance of 0.23 ± 0.39 cm posterior to the EOF/POS (*Table 3*). Its 90th percentiles (total, 0.94 cm; posterior values, 0.98 cm; anterior values, 0.00 cm) indicate a slightly predominant posterior distribution of the lambdoid/sagittal relative to the EOF/POS (*Table 3*).

The Euryon

Because of its palpatory evidence, the craniometric point called the euryon, which corresponds to the center and the most prominent point of the parietal tuberosity (11, 59), was evaluated regarding its cortical-related point through the study of the cortical area underneath the center of a 1.5-cm burr hole centered at the euryon.

The euryon was located over the superior temporal line in three specimen (9%) and just superior to this line in 29 specimen (91%). Relative to a vertical line originating at the mastoid-tip posterior aspect and passing through the parietomastoid suture and squamous suture meeting point, the euryon was anterior to this line in five specimen (16%), at the level of this line in 26 specimen (81%), and posterior to it in one specimen (3%), at an average distance of 0.23 ± 0.75 cm anterior to this vertical line and 6.48 ± 0.79 cm superior to the parietomastoid suture and squamous suture meeting point, without any significant differences between sides in all 32 specimen (*Table 5*). The euryon was situated anterior and inferior to the previously mentioned IPP, at an average distance of 4.10 ± 0.63 cm along an approximately 45-degree inclined line, without significant differences between the right and left sides, in the 28 specimen studied regarding this evaluation (*Table 5*).

The euryon was found to be situated over the superior aspect of the supramarginal gyrus (SMG) in all 32 specimen, more anteriorly located in relation to the SMG middle point in eight specimen (25%), centrally located in nine specimen (28%), and more posteriorly located over the SMG in 15 specimen (47%).

The euryon was posterior to the postcentral sulcus in all 32 specimen, at an average distance of 2.12 ± 0.72 cm. The euryon was lateral to the IPS in all 30 specimen examined for this evaluation, at an average distance of 2.00 ± 0.84 cm, without significant differences between sides. The euryon was anterior to the intermediary sulcus of Jensen (ISJ), which separates the SMG and the angular gyrus (AG), in all 28 specimen studied for this evaluation, at an average distance of 1.36 ± 0.74 cm in the right side and 1.76 ± 0.80 cm in the left side, with a statistically significant difference between sides and with an average value of 1.56 ± 0.78 cm (*Table 5*).

Relative to the posterior sylvian point, the euryon was superior to the posterior sylvian point in all 31 specimen submitted to this verification, having been found to be in the same vertical level of the posterior sylvian point in two specimen (6%) and posterior to the posterior sylvian point in the other 29 specimen (94%). The direct distance between the euryon and the posterior sylvian point had an average value of 2.60 ± 0.66 cm, without significant differences between the right and the left sides (*Table 5*).

TABLE 5. Prominent cranial points and related measurements[a]

	No.			Range	First quartile			Median		
	R	L	Total	Total	R	L	Total	R	L	Total
Eu–post mast/PMS and SqS meeting point vertical line distance	16	16	32	−2.00 to 1.50	0.00	0.00	0.00	0.00	0.00	0.00
Eu-PMS and SqS meeting point distance	16	16	32	5.00 to 8.00	6.00	5.63	6.00	6.50	6.50	6.50
Eu–IPP distance	14	14	28	3.00 to 5.50	3.73	3.50	3.50	4.00	4.00	4.00
Eu–postCS distance	16	16	32	0.50 to 3.70	1.58	1.73	1.73	2.00	2.00	2.00
Eu–IPS distance	14	14	30[b]	0.20 to 3.50	1.43	1.20	1.20	2.35	2.00	2.05
Eu–ISJ distance	14	14	28	0.00 to 3.00	0.75	1.25	1.13	1.60	1.70	1.60
Eu–PSyP distance	15	15	31[b]	1.20 to 4.00	2.50	2.00	2.20	2.70	2.50	2.60
OpCr–CaF distance	13	13	27[b]	−1.00 to 1.00	0.00	0.00	0.00	0.00	0.00	0.00
OpCr–OccBa distance	11	11	24[b]	1.00 to 2.50	1.60	1.20	1.23	2.00	1.70	1.70

The Opisthocranion

The opisthocranion, the craniometric point that corresponds to the most prominent occipital cranial point (11, 59), had its cortical relationships studied through the evaluation of the cortical area situated underneath the center of a 1.5-cm burr hole centered at the opisthocranion level just lateral to the midline.

The opisthocranion was evident in all specimen and was situated at an average distance of 3.00 ± 0.93 cm below the λ (*Table 4*). Relative to the brain surface, it was located at an average distance of 0.05 ± 0.30 cm superior to the distal end of the calcarine fissure among the 27 specimen studied regarding this evaluation (*Table 5*) and at an average distance of 1.71 ± 0.49 cm superior to the most posterior aspect of the occipital base among the 24 specimen studied regarding this evaluation (*Table 5*), in both cases without significant differences between the right and the left sides (*Table 5*). The 90th percentiles pertinent to the opisthocranion and the calcarine fissure positions (total, 0.56 cm; superior values, 0.62 cm; inferior values, 0.00 cm) (*Table 5*) show their close topographical relationship.

DISCUSSION

It is interesting to stress that the neuroimaging and the intraoperative identifications of intracranial structures, as with other body organs, are done from and based on the initial recognition of the surrounding natural spaces, which, intracranially, are constituted by the cerebrospinal fluid–filled spaces, and that surgery is always preferably done through the same natural spaces, and thus also preferably through cerebrospinal fluid spaces for intracranial surgery.

This ideal practice became possible only with the advent of microneurosurgery, particularly with the contributions of M. Gazi Yaşargil (94) and evolved through the progressive development of initial transfissural and transcisternal approaches, particularly for surgery of extrinsic lesions (101) and posterior transsulcal approaches for intrinsic lesions (32, 60, 96, 97, 99), with the consequent establishment of the sulci as fundamental anatomic landmarks for its practice. The brain sulci are now used as surgical corridors for underlying lesions and for reaching the ventricular spaces, for limiting, *en bloc* or piecemeal, resections of intrinsic lesions or gyri and lobules with enclosed lesions, and should be recognized and avoided if necessary.

Given the actual brain anatomy, with the gyri constituting a real continuum throughout their multiple, and, to some extent, also variable, superficial and deep connections that respectively interrupt and limit the depth of their related sulci, it is important to emphasize that despite being distinctively named, the gyri should be understood as arbitrary circumscribed regions of the brain surface, delimited by sulci that correspond to extensions of the subarachnoid space, and that should also be understood as arbitrary circumscribed spaces of the brain surface that can be constituted by single or multiple segments and, to some extent, with a variable morphology (*Fig. 1*).

Once identified at surgery, the brain sulci can be opened and used as microsurgical corridors, or they can be left untouched and used only as anatomic landmarks. Compared with the transgyral approaches, besides the obvious advantage of providing a natural closer proximity to deep spaces and lesions, the transsulcal approaches of the superolateral surface of the brain are naturally oriented towards the nearest part of the ventricular cavity, which can be very helpful when dealing with peri- and/or intraventricular lesions. Despite their anatomic variations, the main sulci have constant topographical relationships with their more closely related ventricular cavities and, thus, with the deep neural structures (32, 54, 64, 75). This unique feature of these sulci's radial orientation relative to the nearest ventricular space is well seen in magnetic resonance imaging (MRI) coronal cuts.

Because the cortex is thicker over the crest of a convolution and thinner in the depth of a sulcus, the transgyral approaches

TABLE 5. Continued

Third quartile			Mean			Standard Deviation			Right × left (Wilcoxon; *P* value)	90th percentiles			Observations
R	L	Total	R	L	Total	R	L	Total		Total	Positive values	Negative values	
0.00	0.00	0.00	−0.31	−0.16	−0.23	0.70	0.81	0.75	0.180				Negative, anterior; positive, posterior
7.00	7.00	7.00	6.53	6.44	6.48	0.83	0.77	0.79	0.477				
4.63	4.50	4.50	4.16	4.04	4.10	0.67	0.60	0.63	0.292				
2.48	2.73	2.50	2.11	2.14	2.12	0.70	0.76	0.72	0.842				
2.58	2.50	2.50	2.08	1.91	2.00	0.90	0.79	0.84	0.349				
1.85	2.63	2.00	1.36	1.76	1.56	0.74	0.80	0.78	0.039[c]				
3.40	2.60	3.00	2.78	2.41	2.60	0.87	0.33	0.66	0.116				
0.00	0.00	0.00	0.10	−0.04	0.05	0.38	0.14	0.30	0.180	0.56	0.62	0.00	Negative, inferior; positive, superior
2.00	2.40	2.00	1.77	1.73	1.71	0.45	0.54	0.49	0.765				

[a] R, right; L, left; Eu, euryon; post mast, posterior aspect of the mastoid process; PMS and SqS meeting point, parietomastoid and squamous sutures meeting point; IPP, intraparietal point; postCS, postcentral sulcus; IPS, intraparietal sulcus; ISJ, intermediary sulcus of Jensen (sulcus between the supramarginal and the angular gyri); PSyP, posterior sylvian point; OpCr, opisthocranion; CaF, calcarine fissure; OccBa, occipital base. Measurements are in centimeters.
[b] Different total number due to inclusion of nonpaired specimen, as explained in the Patients and Methods section.
[c] Significant difference between the left and right sides.

sacrifice a bigger number of neurons and projection fibers, whereas the transsulcal approaches sacrifice a bigger number of U fibers (14, 32, 88).

The transsulcal approach's major disadvantage is that the surgeon has to deal with intrasulcal vessels with diameters proportional to the sulci dimensions and with occasional cortical veins that can run along the sulci surface. Besides their respective vascular impairments, the damage of these vessels can cause bleeding that can spread through the adjacent subarachnoid space and that can obliterate the proper microsurgical view. Even small vessels can be critical in eloquent areas of the brain.

To avoid stretching and/or tearing these vessels, and to optimize the sulci opening, the arachnoid should be divided, preferably with sharp instruments, and the sulci should be progressively opened at a similar depth level along its entire required extension. The running arteries should be freed and protected towards one side after the coagulation and division of their tiny contralateral perforating branches, and whereas the coagulation and division of bigger veins are conditioned to their locations, the small intrasulcal veins should be usually coagulated to prevent posterior bleeding during subsequent maneuvers; vessels at the sulci depth can be avoided if necessary by entering the white matter before them. Bigger sulcal opening extensions provide less traction of the sulcal-related vessels and walls, easing the transsulcal work by decreasing the need for still retractors.

For hemispheric intrinsic lesion removal, the transsulcal approaches can be useful for reaching lesions that can then be removed piecemeal or *en bloc*, and also for delimiting the removal of a gyral region that encloses the lesion. Particularly for the infiltrative gliomas that frequently remain confined within their sites of origin for some time (96), the anatomic removal of a gyral or a lobular sector enclosing the tumor is justified and can facilitate and enhance its radical resection in noneloquent areas.

Parallel to the significant microneurosurgical (94) and intracranial microanatomic knowledge (64, 95, 96) developments of the past decades, it is interesting to observe that the current localization of the brain sulci and gyri on the external cranial surface for the proper positioning of supratentorial craniotomies and for general transoperative orientation (65, 75, 86) is still mostly based in cranial–topographic anatomy studies done particularly during the second half of the 19th century (9, 28, 38, 39, 42, 83, 84, 86), or done with the aid of stereotactic (15) or sophisticated frameless imaging devices (90).

The personal appraisal of the surface projection of intrinsic lesions seen in neuroradiological images frequently done by neurosurgeons is difficult and not secure because of the irregular oval shape of the skull and the brain, the obliqueness and variable levels of axial and coronal images, and the lack of fine cranial vault imaging in MRI 3-D reconstructions. Special techniques developed for this aim may require specific devices and are based on calculations that are not free of error (16, 27, 33, 37, 41, 52, 58).

The intraoperative frameless imaging devices developed during the past decade (90), when available, are no substitute for the cranial–cerebral anatomic knowledge that every neurosurgeon must have and must improve throughout his or her practice. Moreover, the transoperative brain displacement can affect the accuracy of these navigation systems (18, 68, 81), and although real-time corrections can be made through the fusion of ultrasound images with neuronavigation (87), a proper transoperative anatomic orientation is, of course, mandatory for interpreting and double-checking these imaging data. The same can be argued about the more recent development of

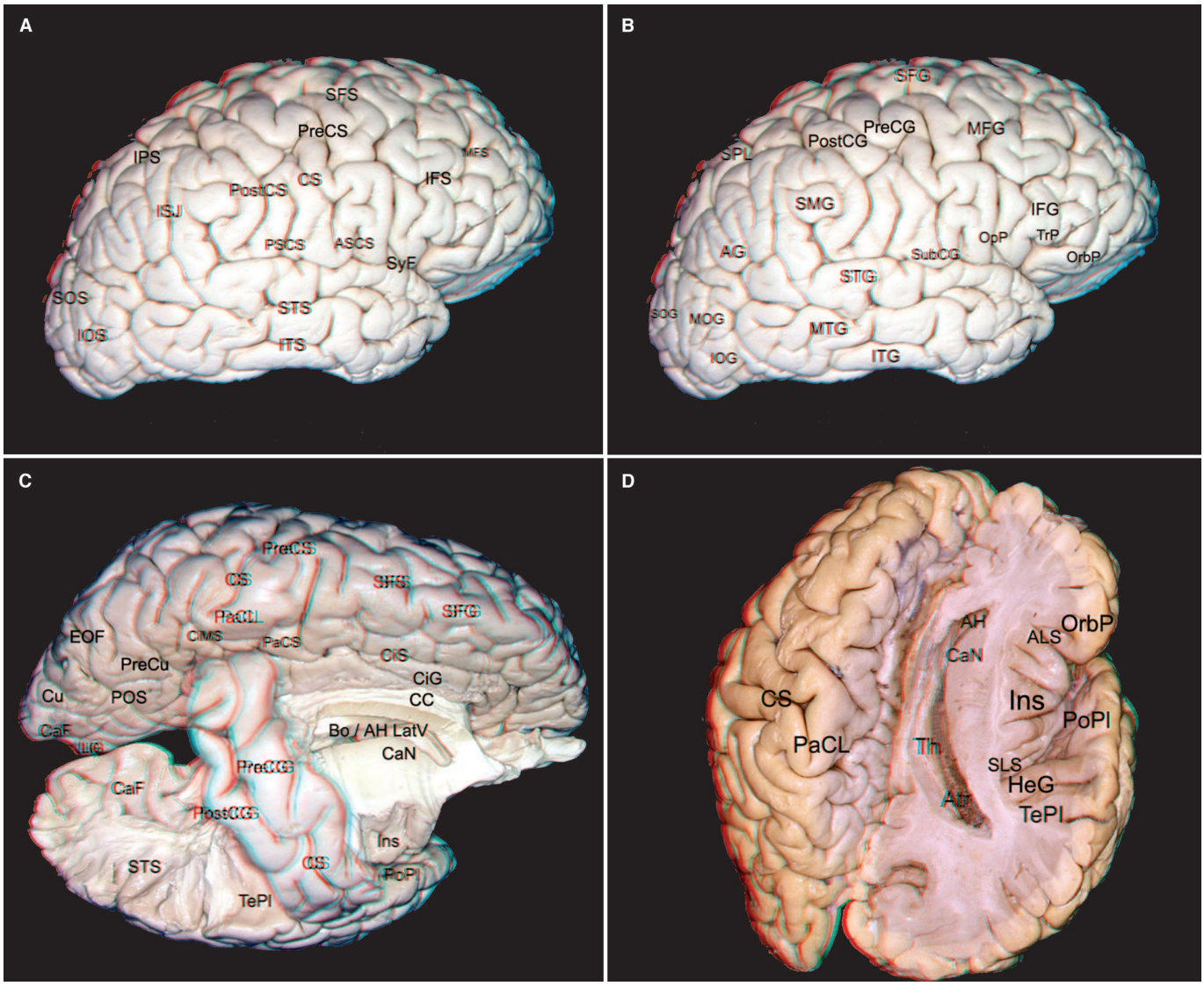

FIGURE 1. *Sulci and gyri of the superolateral face of the brain and their relationships with the cerebral structures and lateral ventricles.* A *and* B, *main sulci and gyri of the superolateral face of the brain. The SFS and the IFS sulci, respectively, separate the SFG, MFG, and IFG, with the latter being constituted by the orbital* (OrbP)*, triangular* (TrP)*, and opercular* (OpP) *parts. Within the SFG, there is usually a shallow sulcus called a medial frontal sulcus (54) (not shown in the figure), and enclosed within the MFG, there is frequently also a secondary intermediate sulcus (54), or middle frontal sulcus* (MFS)*. Similarly, the STS and the inferior temporal sulci* (ITS) *divide the superior* (STG)*, middle* (MTG)*, and inferior* (ITG) *temporal gyri, and the superior occipital sulcus* (SOS) *and inferior occipital sulcus* (IOS) *(50) divide the less defined superior* (SOG)*, middle* (MOG)*, and inferior* (IOG) *occipital gyri. Approximately in the middle of the superolateral surface of the brain, the precentral gyrus and the postCG are obliquely disposed just above the sylvian fissure as a long ellipse excavated by the usually continuous CS, being connected along the superior end of the CS by the superior frontoparietal plis de passage of Broca, or paracentral lobule, already in the mesial surface of the brain (not shown in the figure) and connected below the CS by the inferior frontoparietal plis de passage, also called rolandic operculum and subCG, which is anteriorly and posteriorly delimited by the small sylvian fissure branches' anterior* (ASCS) *and posterior* (PSCS) *subcentral sulci. The precentral gyrus is anteriorly bound by the precentral sulcus, which is usually interrupted, particularly by a connection between the precentral gyrus and the MFG. Inferiorly, the precentral sulcus ends inside the U-shaped IFS OpP. The postcentral sulcus delimits the posterior aspect of the postCG. The IPS divides the parietal lobe in the superior parietal lobule* (SPL)*, which is medially continuous with the precuneus gyrus (not shown in the figure) and in the inferior parietal lobule that is composed by the SMG and the AG. Anteriorly, the usually curvilinear IPS is generally continuous with the inferior half of the postcentral sulcus; posteriorly, it is generally continuous with the SOS (84), which is also called the intraoccipital (19, 50) and transverse occipital sulcus (54). Whereas the SMG encloses the distal end of the sylvian fissure, thus becoming inferiorly continuous with the STG, the AG usually contains an inferior distal branch of the STS, and both gyri are separated by a single or double sulcus (i.e., the ISJ) (90), which can be an inferior perpendicular branch of the IPS and/or constituted by the superior distal branch of the STS.* C, *precentral gyrus*

intraoperative MRI (4, 5, 92) and even about any forthcoming neurosurgical instrument or imaging possibilities, such as the recent magnetic resonance axonography (17, 36, 40, 61, 93), in that the planning, practice, and evaluation of any surgical procedure intrinsically require a proper anatomic knowledge and can be particularly enhanced by its tridimensional understanding. Although extremely useful and more precise than any method based on anatomic correlations, the navigation systems are not available in many countries around the world because of their cost, and the stereotactic systems are not practical enough for daily use in usual cases.

Regarding the functional reliability of using anatomic sulcal and gyral landmarks for microneurosurgical orientation, it is necessary to consider that the studies of functional neuroimaging and intraoperative cortical stimulation denote findings that, in general, corroborate the expected relationships between elicited functional responses and their respective eloquent anatomic sites, just as these can be morphologically identified through neuroimaging and, eventually, during surgery itself (2, 7, 8, 20, 23, 29, 45, 53, 62, 70, 72, 78, 86, 105). On the other hand, any transoperative anatomic identification of any eloquent cortical area, even when confirmed by a localizing imaging system, cannot safely substitute for the aid of transoperative functional or neurophysiological testing because of possible anatomic functional variations and their possible displacements and/or involvement by the underlying pathology (23, 53, 78, 86).

The Concept of Sulcal and Gyral Key Points and Their Cranial–Cerebral Relationships

The microneurosurgical importance of the sulci and their notorious difficulty to be identified during regular neurosurgical procedures justified the study of sulcal and gyral key points and their cranial–cerebral topographical correlations to aid their surgical identification. The essential microsurgical sulcal and cortical key points to be studied were those constituted by the main sulci extremities and/or intersections, and by the gyral sites that underlie particularly prominent cranial points (*Figs. 2* and *3*). On the superolateral surface of the brain, besides the CS, the precentral sulcus, the postcentral sulcus, and the always evident sylvian fissure, the other main sulci are the SFS, the IFS, the STS, and the IPS.

In addition to the CS extremities, the small distances that were found in the present study between the SFS posterior extremity and the precentral sulcus (0.69 ± 0.56 cm) and between the IFS posterior extremity and the precentral sulcus (0.03 ± 0.48 cm), as well as the usual continuity between the IPS and the postcentral sulcus (83%), warrant these real or virtual sulcal interconnections to be considered as distinguished sulcal key points for practical neurosurgical purposes. Given their anatomic regularities and their surgical importance, the superior extremity of the POS that corresponds to the medial extremity of the EOF, the posterior portion of the STS, the SMG point that underlies the center of the parietal prominence (euryon), and the distal end of the calcarine fissure that underlies the occipital prominence (opisthocranion) were also studied here as important sulcal and gyral key points.

Together, these sulcal and gyral key points, with their corresponding cranial points, constitute a neurosurgical anatomic framework that can be used to orient the placement of supratentorial craniotomies and to ease the initial transoperative identification of brain sulci and gyri.

Considering the previously mentioned difficulties in projecting a subcortical lesion seen on MRI images on the cranial surface for planning a proper craniotomy, and as with the navigation systems that localize any given point according to its position relative to points with previously known coordinates, with the aid of these key points, any intrinsic cerebral lesion can be 1) initially understood regarding the structure and/or the intracranial space that contains the lesion and 2) have its external cranial projection estimated based on the position of its most related cortical and sulcal key points and their corresponding cranial points. In addition, to propitiate the external projection of the lesion, its most related sulcal key

←

FIGURE 1. (Continued) *and postCG, which constitute the central lobe (96), are disposed as an inclined fan on the top of the thalamus (*Th*) and relative to its related neural structures and spaces, whereas the inferior aspect of the central lobe covers the posterior half of the insula (*Ins*), constituting the rolandic operculum with the postCG disposed over the HeG. Its superior aspect overlies the atrium (*Atr*) of the lateral ventricle (*LatV*).* D, *axial view at the SLS level discloses that the Ins covers the basal ganglia, the Th, and the internal capsule as a shield, with its anterior half being particularly related to the head of the caudate nucleus (*CaN*) and its posterior half to the Th, which, respectively, are related to the lateral ventricle AH and to the body and Atr. Whereas the ALS points to the AH, the posterior aspect of its SLS points to the Atr. The HeG divides the temporal operculum in the oblique PoPl, which that actually covers the Ins, and in the triangular and flat TePl, which, together with the HeG, point to the Atr. Regarding the central lobe, as also implied in* C, *the PaCL is topographically related with the Th and the ventricular Atr, and the postCG lies over the HeG, with its posterior SMG resting over the TePl.* AG, *angular gyrus;* AH, *anterior horn;* ALS, *anterior limiting sulcus of the insula;* ASCS, *anterior subcentralsulcus;* Atr, *atrium of lateral ventricle;* Bo/AHLatV, *body and anterior horn of lateral ventricle;* CaF, *calcarine fissure;* CaN, *caudade nucleus;* CC, *corpus callosum;* CiG, *cingulate gyrus;* CiMS, *cingulate sulcus marginal ramus;* CiS, *cingulate sulcus;* CS, *central sulcus;* CU, *cuneus;* HeG, *Heschl gyrus;* IFG, *inferior frontal gyrus;* IFS, *inferior frontal sulcus;* IOG, *inferior occipital gyrus;* IOS, *inferior occipital sulcus;* Ins, *insula;* IPS, *intraparietal sulcus;* ITG, *inferior temporal gyrus;* ITS, *inferior temporal sulcus;* MFG, *middle frontal gyrus;* MFS, *middle frontal sulcus;* MOG, *middle occipital gyrus;* MTG, *middle temporal gyrus;* OpP, *opercular part;* OrbP, *orbital part;* PaCL, *paracentral lobule;* PaCS, *paracentral sulcus;* PoPl, *polar planum;* PostCG, *postcentral gyrus;* PostCS, *postcentral sulcus;* PreCG, *precentral gyrus;* PreCS, *precentral sulcus;* PreCu, *precuneus;* PSCS, *posterior subcentral sulcus;* SFG, *superior frontal gyrus;* SFS, *superior frontal sulcus;* SLS, *superior limiting sulcus of the insula;* SMG, *supramarginal gyrus;* SOG, *superior occipital gyrus;* SOS, *superior occipital sulcus;* SPL, *superior parietal lobule;* STG, *superior temporal gyrus;* STS, *superior temporal sulcus;* SubCG, *subcentral gyrus;* SyF, *sylvian fissure;* TePl, *temporal planum;* Th, *thalamus;* TrP, *triangular part.*

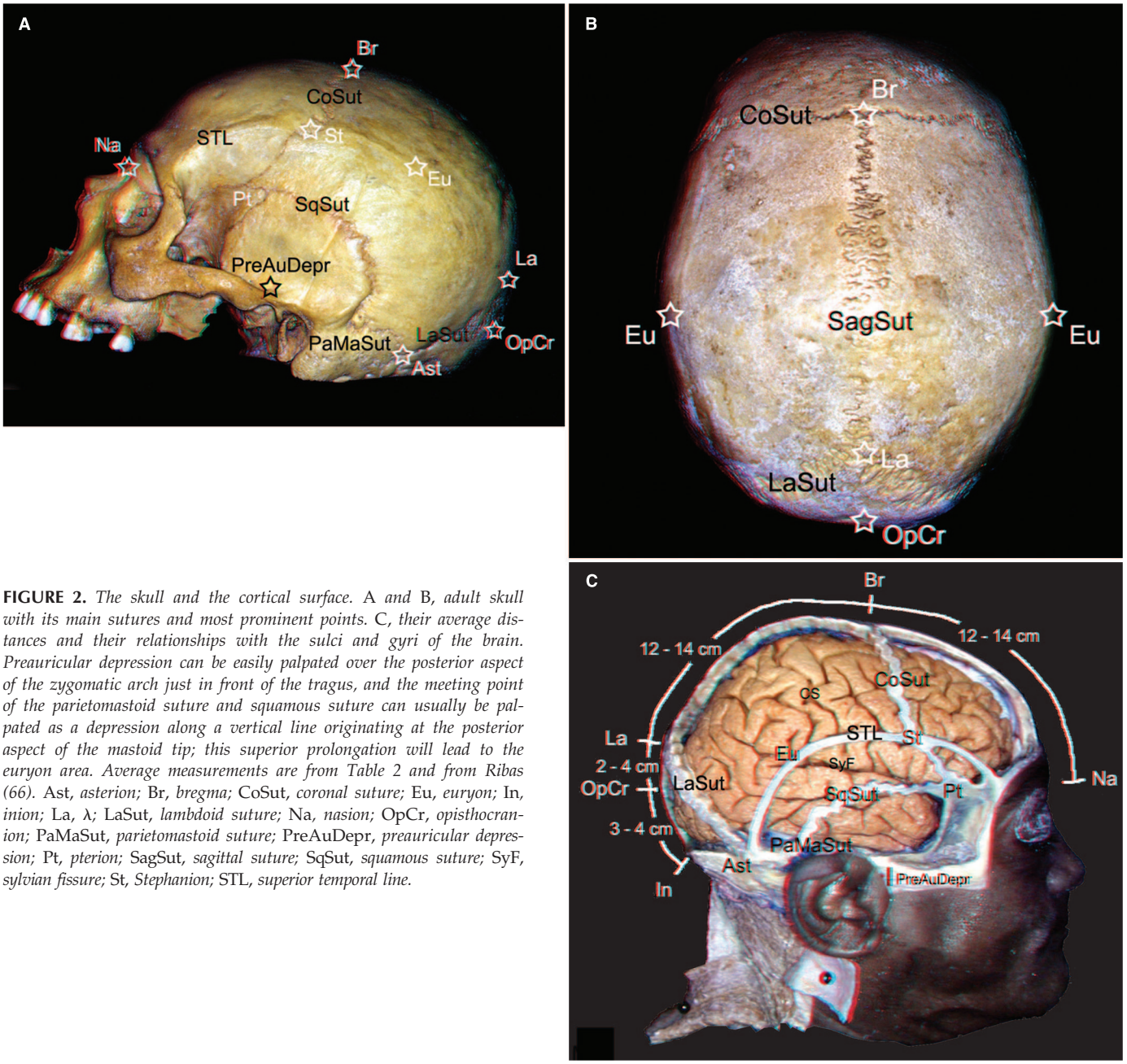

FIGURE 2. *The skull and the cortical surface.* A *and* B, *adult skull with its main sutures and most prominent points.* C, *their average distances and their relationships with the sulci and gyri of the brain. Preauricular depression can be easily palpated over the posterior aspect of the zygomatic arch just in front of the tragus, and the meeting point of the parietomastoid suture and squamous suture can usually be palpated as a depression along a vertical line originating at the posterior aspect of the mastoid tip; this superior prolongation will lead to the euryon area. Average measurements are from Table 2 and from Ribas (66).* Ast, *asterion;* Br, *bregma;* CoSut, *coronal suture;* Eu, *euryon;* In, *inion;* La, *λ;* LaSut, *lambdoid suture;* Na, *nasion;* OpCr, *opisthocranion;* PaMaSut, *parietomastoid suture;* PreAuDepr, *preauricular depression;* Pt, *pterion;* SagSut, *sagittal suture;* SqSut, *squamous suture;* SyF, *sylvian fissure;* St, *Stephanion;* STL, *superior temporal line.*

points will also serve as natural references pertinent to the best transsulcal or transgyral approach for the target lesion, thus further contributing to the proper placement of the required craniotomy.

According to our findings, the sulcal key points studied here can be intraoperatively identified within an interval of up to 2 cm relative to their related cranial points, aided by the fact that the sulcal key points are usually visually characterized by a certain degree of enlargement of the subarachnoid space because they generally correspond to an intersection of two sulci. The surgeon's knowledge of the usual shape and most frequent anatomic variations of the main brain sulci (54, 96) helps to corroborate his or her identification of these sulci, and their key points' cisternal aspects can then enhance their characterization as microsurgical dissection starting points and/or as limiting surgical boundaries.

Considering the dimensions of the usual craniotomies and the usual cortical exposures that can be further examined through surgical microscopes, an interval range of up to 2 cm between the sulcal key points and their related cranial points was considered

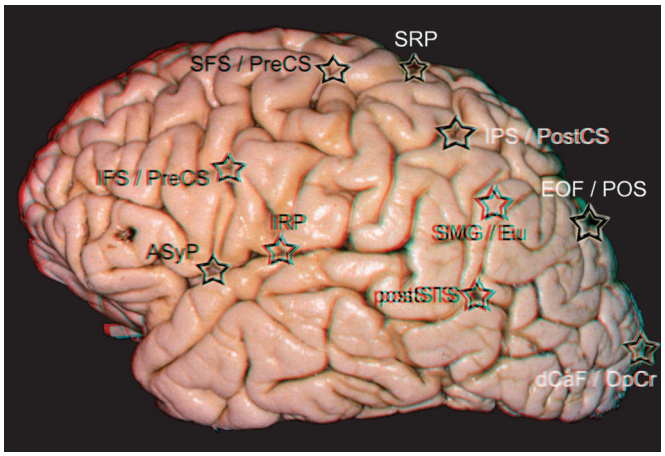

FIGURE 3. *Microneurosurgical sulcal/cortical key points. The microneurosurgical key points of the brain surface are constituted by real intersections between adjacent sulci or by their prolongations and by gyral and sulcal points located underneath prominent skull points such as the euryon (center of the parietal tuterosity) and the opisthocranion (most prominent occipital point). Note that the sulci meeting points are usually characterized by an enlargement of the subarachnoid space.* Eu, *euryon;* OpCr, *opisthocranion;* ASyP, *anterior sylvian point;* dCaF/OpCr, *distal calcarine fissure point, underneath the opisthocranion;* EOF/POS, *external occipital fissure medial point, equivalent to the most superior point of the parieto-occipital sulcus in the medial surface of the brain;* IFS/PreCS, *inferior frontal sulcus and precentral sulcus meeting point;* IPS/PostCS, *intraparietal sulcus and postcentral sulcus transitional or meeting point;* IRP, *inferior Rolandic point;* postSTS, *superior temporal sulcus posterior segment and extremity;* SFS/PreCS, *superior frontal sulcus and precentral sulcus meeting point;* SMG/EU, *superior aspect of the supramarginal gyrus disposed underneath the Euryon;* SRP, *superior Rolandic point.*

acceptable for the surgical purposes of craniotomy placement and the intraoperative visual identification of sulcal key points. The rare statistically significant differences between the right and the left sides were all pertinent to differences of measurements far below this 2-cm margin of error.

Frontotemporal Key Points

Anterior Sylvian Point

The sylvian fissure is the most identifiable feature of the superolateral face of the brain, and, since Yaşargil et al.'s (101) original description of the microsurgical anatomy of the subarachnoid cisterns in 1976, it has constituted the main microneurosurgical corridor to the base of the brain (95, 96, 99, 100, 102). The sylvian fissure is divided into a proximal segment (stem, sphenoidal, anterior ramus) and a distal segment (lateral, posterior ramus) separated by the sylvian point (85, 102). In the present study, the sylvian (98) point is designated as the anterior sylvian point in opposition to the posterior distal sylvian point that corresponds to the distal extremity of the sylvian fissure posterior ramus and that originates the ascending terminal ramus and the occasional descending terminal ramus (54).

The anterior sylvian point's constant location and its cisternal aspect, which has already been exhibited in older illustrations (39, 83) and in recent publications (19, 40, 54, 59, 64, 74, 75, 79, 82, 85, 95, 96, 102), suggest that the anterior sylvian point could be used not only as a starting site to open the sylvian fissure, but also as an initial landmark to intraoperatively identify other important neural and sulcal structures that are usually hidden along the fissure by its arachnoidal and vascular coverings; these features characterize the anterior sylvian point as the prototype of a microneurosurgical sulcal key point. Its usually evident morphological cisternal aspect, which is attributable to an enlargement of the sylvian fissure caused by the usual retraction of the IFG's triangular part in relation to the sylvian fissure, was seen in 94% of our samples (*Fig. 4*).

Yaşargil et al. (103) emphasize that "the sylvian point is located in the same plane of the IFG triangular part, and 10 to 15 mm anterior to the sylvian venous confluence constituted by frontal and temporal tributaries veins" and advises "to begin opening the fissure immediately anterior to this vein confluence at a point where a temporal or frontal artery or where both arteries appear at the surface of the fissure," that is, at the anterior sylvian point area.

Inferior Rolandic Point

The CS inferior extremity was found to be either just above the sylvian fissure (83%) or inside the sylvian fissure (17%), and its small distance from this fissure (average distance, 0.54 $\pm$ 0.62 cm superior to the sylvian fissure, 90th percentile, 1.20 cm) justified the study of the real or virtual CS and sylvian fissure intersection site as a single microsurgical key point, the IRP (83) (*Fig. 4*).

The IRP has an obvious neurosurgical importance, and its location along the sylvian fissure can be intraoperatively estimated as being situated 2.36 $\pm$ 0.50 cm posterior to the visually evident anterior sylvian point according to our findings.

Regarding its cranial relationships, our results show that the IRP lies underneath the point of intersection of the squamous suture with a vertical line originating in the preauricular depression, which is situated immediately above the zygoma and in front of the tragus, within an excellent vertical relationship and horizontally with a slightly predominant posterior distribution, within an interval below 2 cm (*Table 4*). This site corresponded in all cases to the higher segment of the squamous suture (average, 0.08 $\pm$ 0.41 cm above the squamous suture, 90th percentile, 0.46 cm; average, 0.06 $\pm$ 1.01 cm posterior to the squamous suture, 90th percentile, 1.16 cm), which relates this higher squamous segment with the precentral gyrus and postcentral gyrus (postCG) inferior connection (subcentral gyrus, inferior Broca's frontoparietal *plis de passage*. The knowledge of the average vertical height of this segment of the squamous suture from the preauricular depression of 4 cm can help in estimating its external cranial position (*Table 4*).

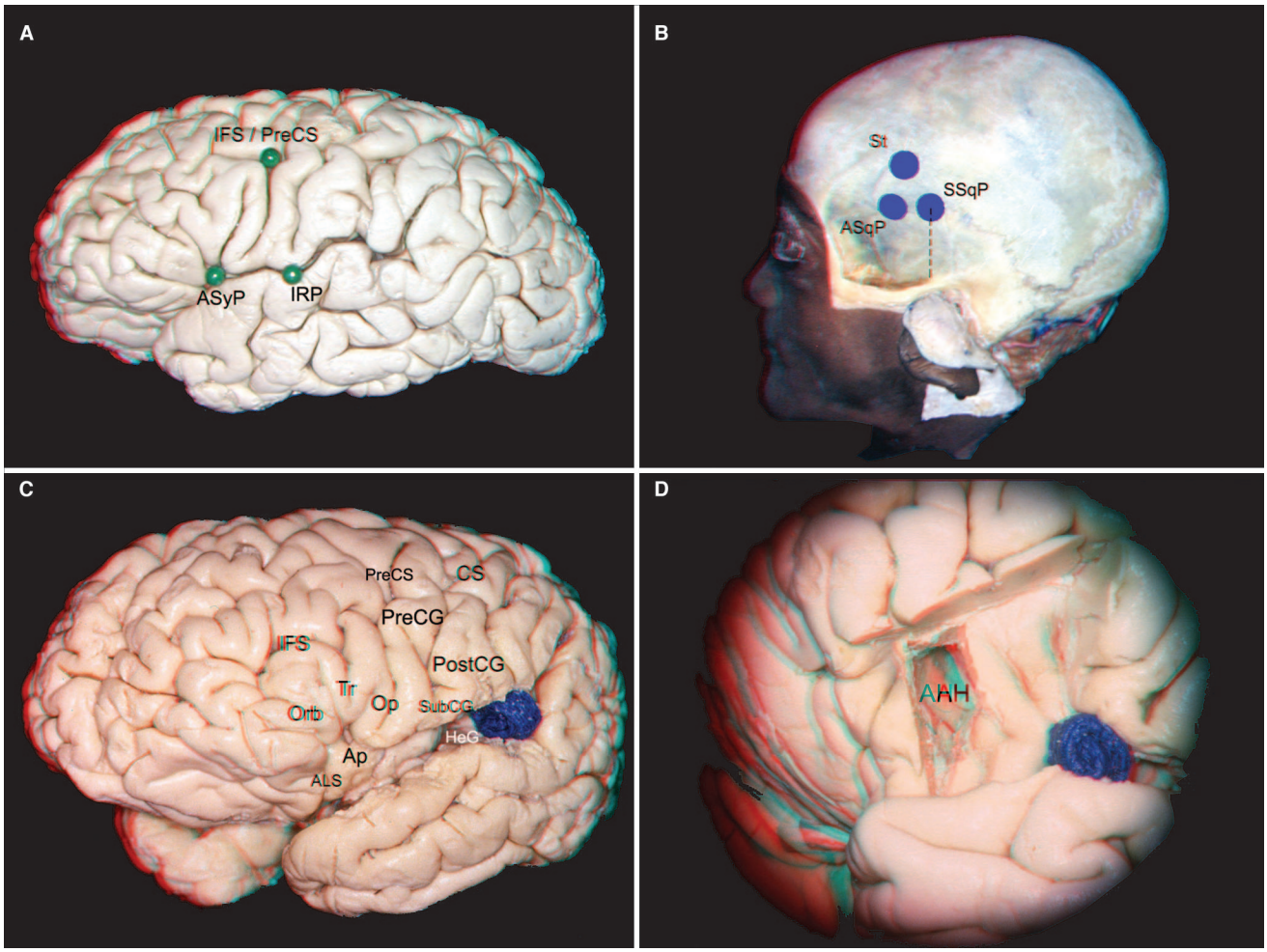

FIGURE 4. *Frontotemporal key points.* A, *the frontal and temporal sulci and gyri topography can be estimated through the identification of the anterior sylvian point, IRP, and IFS/precentral sulcus. The anterior sylvian point is characterized by enlargement of the sylvian fissure inferior to the triangular part* (Tr) *and anterior to the opercular part* (Op) *of the IFG and serves particularly as an appropriate starting point for the sylvian fissure opening. The IRP corresponds to the CS inferior extremity projection onto the sylvian fissure and is situated approximately 2 to 3 cm posterior to the anterior sylvian point. The IFS/precentral sulcus indicates the height of the IFS Op and delineates the anterior aspect of the precentral gyrus at the face motor activation area (57).* B, *regarding their cranial–cerebral relationships, the anterior sylvian point is located underneath the anterior squamous point, just posterior to the pterion. The IRP is usually located underneath the highest superior squamous point, which is indicated by a* vertical dotted line *originating at the preauricular depression. The IFS/precentral sulcus is located underneath the St cranial area, which corresponds to the site of intersection of the coronal suture with the superior temporal line.* C, *the wide opening of the sylvian fissure discloses the insular apex located at the anterior sylvian point coronal level, just posterior to the ALS. Just posterior to the IRP, the opercular surface of the PostCG lies on the HeG.* D, *The depth of the most superior aspect of the insular ALS is closely related with the lateral ventricle AH. This part of the AH is constituted by a ventricular recess located just anterior to the head of the caudate nucleus and is separated from the ALS depth by the fibers of the internal capsule anterior limb.* AH, *lateral ventricle anterior horn;* ALS, *anterior limiting sulcus of the insula;* Ap, *apex of the insula;* ASqP, *anterior squamous suture point, over ASyP;* ASyP, *anterior Sylvian point;* CS, *central sulcus;* IFS, *inferior frontal sulcus;* HeG, *Heschl gyrus;* IFS/PreCS, *inferior frontal and precentral sulci meeting point;* IRP, *inferior rolandic point;* Op, *inferior frontal gyrus opercular part;* Orb, *inferior frontal gyrus orbital part;* PostCG, *postcentral gyrus;* PreCG, *precentral gyrus;* PreCS, *precentral sulcus;* SSqP, *superior squamous point, over IRP;* St, *Stephanion, over IFS/PreCS;* SubCG,*subcentral gyrus (pre- and postcentral gyri inferior connection arm);* Tr, *inferior frontal gyrus triangular part.*

It is interesting to note that other authors also related the CS inferior extremity with the same vertical line originating at the preauricular depression, but none of them studied the relationship of the CS inferior extremity projection over the sylvian fissure with the squamous suture level. Poirier described the lower extremity of the CS as being situated over a line perpendicular to the zygomatic arch and located immediately anterior to the tragus, 7 cm superior to the preauricular point that frequently can be characterized as an evident small depression just anterior to the tragus (84). In 1900, Taylor and Haughton (83) described the inferior extremity of the CS as being situated in the intersection of this same perpendicular

line with the so-called sylvian line, which these authors defined as a line drawn from the junction of the third and fourth 0segments of the nasion–inion (In) curve to the orbitotemporal angle. Championniere positioned the IRP 3.5 cm superior to the posterior extremity of a 7-cm line parallel to the zygomatic arch and initiated at the frontozygomatic point that corresponds to the site of the frontozygomatic suture situated on the lateral orbital rim (84). Recently, Rhoton (64) mentioned that the IRP is located approximately 2.5 cm posterior to the pterion on the sylvian fissure line, which corresponds to a line drawn between the frontozygomatic point and the three-quarter point of the nasion in distance.

The Inferior Frontal and Precentral Sulcus Meeting Point

The IFS can end in connection with the precentral sulcus or very close to this sulcus (average distance: anterior, 0.03 ± 0.48 cm, 90th percentile, 0.61 cm), and their connection point, or the point of connection of an IFS prolongation line with the precentral sulcus when they don't actually connect, designated here as the IFS and precentral sulcus meeting point (IFS/precentral sulcus), is a practical neurosurgical key point that 1) delineates anteriorly the precentral gyrus at its inferior third level, which corresponds to the face motor activation area (56, 57) and 2) indicates the posterior and superior limits of the IFG opercular part (*Fig. 4*).

Evaluation of the IFS/precentral sulcus key point cranial relationships indicates that this point lies underneath the coronal suture and the superior temporal line meeting point, which corresponds to the craniometric point stephanion (St) (10) within a safe interval very much below 2 cm (St located 0.17 ± 0.50 cm inferior to IFS: 90th percentile, 0.00 cm; and 0.34 ± 0.71 cm anterior to precentral sulcus: 90th percentile, 0.68 cm). Its topographic relationship with the IFS had already been showed by Broca (11) and Seeger (74), clearly relating the inferior aspect of the coronal suture with the inferior aspect of the precentral sulcus.

Frontotemporal Craniotomies

Frontotemporal exposures are currently based in the pterional or frontotemporosphenoidal craniotomy described by Yaşargil (95, 100) and probably constitute the most commonly used and systematized neurosurgical procedure.

Our findings pertinent to the frontotemporal sulcal key points and their corresponding cranial sites can be of some help in identifying the perisylvian sulci and convolutions in preoperative radiological images, and intraoperatively in placing proper craniotomies. Whereas these sulcal key points can help in the radiological and intraoperative identification of the perisylvian sulci and gyri, their corresponding cranial sites can aid in the proper placement of frontotemporal craniotomies, particularly regarding their posterior extensions (*Fig. 5*).

With cortical exposure, the anterior sylvian point can usually be easily recognized because of its cisternal aspect. According to our findings, the IRP is located 2 to 3 cm posterior to the anterior sylvian point, along the sylvian fissure. Considering the average measurements between the anterior sylvian point and the posterior sylvian point, the IRP is situated along the middle third of the horizontal or posterior sylvian fissure segment (54). Because the PostCG opercular aspect lies over the Heschl gyrus (HeG) (91), the IRP also indicates the position of the anterior margin of the HeG along the sylvian fissure, and hence the limit between the polar (PoPl) and the temporal planum (TePl) of the temporal opercular surface.

Because the posterior segment of the IFS and the IFS/precentral sulcus key point bound the superior limit of the IFG opercular part (height from the sylvian fissure, 2.84 ± 0.65 cm) and point to the face area of the precentral gyrus, together with the anterior sylvian point and the IRP, they can constitute important landmarks for intraoperatively estimating the core of Broca's area in the dominant hemisphere and for guiding restricted removals of the inferior portion of the motor strip, which is safer in the nondominant hemisphere and occasionally necessary in vascular, tumor, and epilepsy surgery (31).

Considering that the IRP indicates the position of the HeG, removal of the superior and middle temporal gyri posterior to the IRP in the dominant hemisphere enhances the risk of permanent dysphasia (31, 63).

Superior Frontal and Central Key Points

The Superior Frontal and Precentral Sulci Meeting Point

Given its usual constancy, straightness, depth, and its reliable relationship with the underlying ventricular frontal horn, the SFS constitutes an important microneurosurgical corridor (32). Its posterior extremity, which usually joins or lies very close to the precentral sulcus (average distance, posterior 0.69 ± 0.56 cm; 90th percentile, 1.50 cm), is an important key point that delineates anteriorly the precentral gyrus at the level of its hand motor activation area (7, 105) and limits posteriorly the SFS opening (*Fig. 6*).

The point that was designated in this study as the superior frontal and precentral sulci meeting point (SFS/precentral sulcus) was found to be close to the midline (average distance, 2.67 ± 0.37 cm), at a similar distance found by Harkey et al. (32) (mean, 27 mm; range, 22–35 mm from the midline). Anterior to the SFS/precentral sulcus, the SFS is systematically parallel to the IHF and is usually characterized as a significant continuous segment (average, 5.74 ± 2.62 cm).

Considering its relationships along its coronal plane level, the SFS/precentral sulcus meeting point constitutes an important microsurgical landmark for both the superior frontal transsulcal and the interhemispheric transcallosal approaches to the ventricular cavity because the SFS/precentral sulcus key point was found in all cases to be coronally related with the superior surface of the thalamus and, thus, with the floor of the lateral ventricle body, just behind the foramen of Monro.

Analysis of our findings regarding the SFS/precentral sulcus meeting point cranial relationships indicates that this important frontal sulcal key point lies underneath the cranial point located 3 cm lateral to the sagittal suture and 1 cm posterior to the coronal suture, below the 2-cm accepted error interval (distance from this cranial point to SFS: medially 0.07 ± 0.32 cm, 90th percentile: 0.44 cm; to precentral sulcus anteriorly 0.76 ± 0.79 cm, 90th percentile: 0.00 cm).

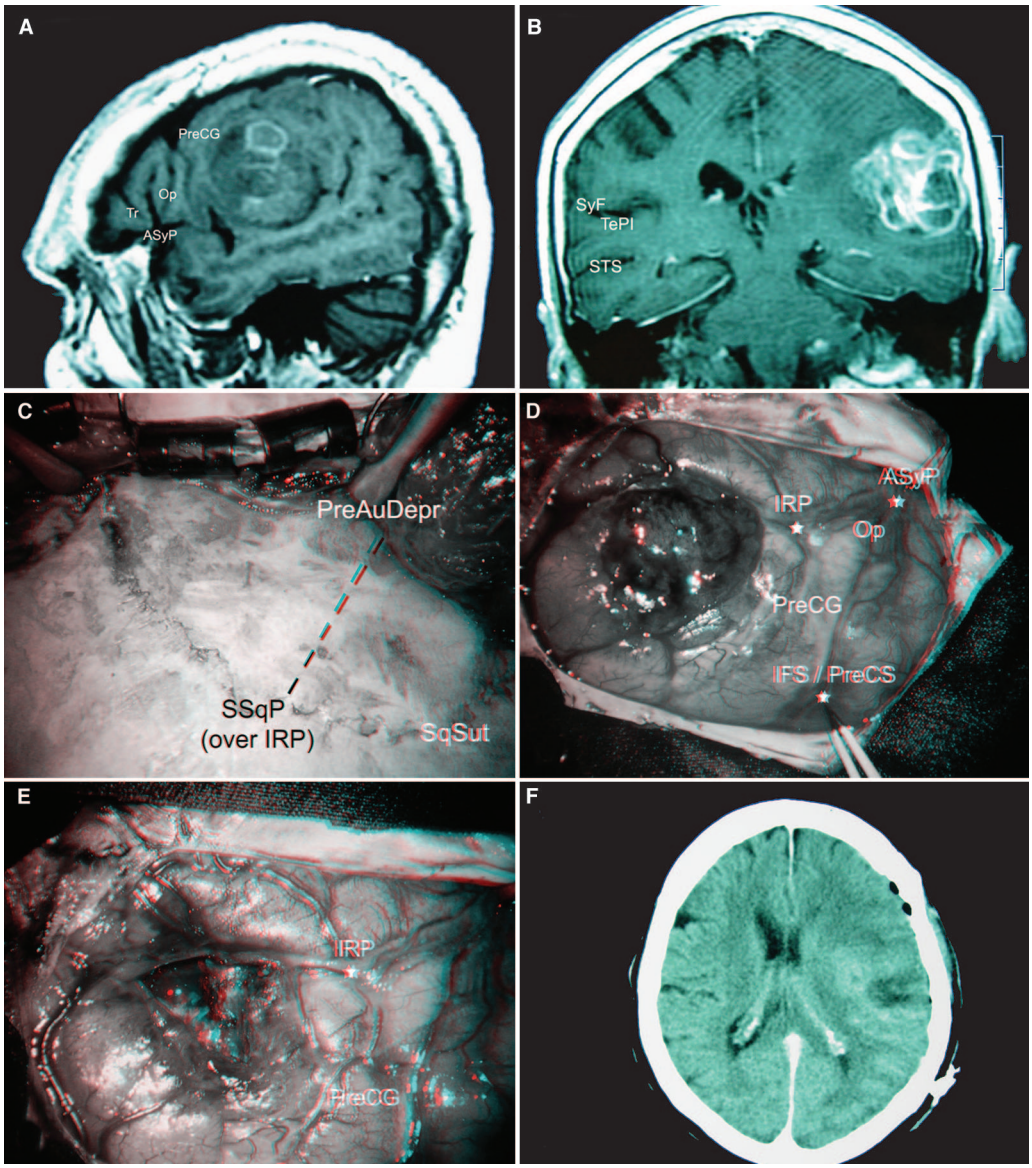

FIGURE 5. *Frontotemporal craniotomy for exposure of the suprasylvian operculum.* A, *sagittal MRI scan of a glioblastoma multiform within the inferior aspect of the PostCG of a 75-year-old woman without focal deficits.* B, *coronal MRI scan showing the tumor over the flat aspect of the distal sylvian fissure that corresponds to the temporal plane.* C, *patient in the lateral position and intraoperative identification of the most superior aspect of the superior squamous point, which corresponds to the intersection site between the squamous suture and a vertical line originating at the preauricular depression and overlying the IRP.* D, *exposure of the suprasylvian operculum through a frontotemporal craniotomy centered at the most superior segment of the superior squamous point, and identification of the IRP, anterior sylvian point, and the IFS and precentral sulcus meeting point (IFS/precentral sulcus), which enable estimation of the topography of their related sulci and gyri.* E, *surgical image and* (F) *CT scan image after the PostCG glioblastoma multiform debulking.* ASyP☆, *anterior sylvian point;* IFS/PreCS☆, *inferior frontal and precentral sulci meeting point;* IRP☆, *inferior rolandic point;* Op, *inferior frontal gyrus opercular part;* PreAuDep, *preauricular depression;* PreCG, *precentral gyrus;* SqSut, *squamous suture;* SSqP, *superior squamous point, over IRP;* STS, *superior temporal sulcus;* SyF, *sylvian fissure;* TePl, *temporal planum;* Tr, *inferior frontal gyrus triangular part.*

It should be emphasized that the SFS posterior extremity points to the precentral gyrus at the hand motor activation area as shown by Boiling et al. (7) and Yousry et al. (105), respectively, with positron emission tomography and functional magnetic resonance imaging studies. Yousry et al.'s (105) intraoperative direct motor mapping findings that the hand motor area is located 30 to 45 mm (mean, 39 mm) from the sagittal suture and 18 to 35 mm (mean, 27 mm) from the coronal suture particularly corroborate our suggestion that the SFS/precentral sulcus key point, located 1 cm posterior to the coronal suture and 3 cm lateral to the sagittal suture, should be considered the posterior limit of the SFS opening and of the frontal interhemispheric retraction for anterior transcallosal approaches to the body and to the anterior horn of the lateral ventricle, still with a safe margin of error.

These findings are in accordance with text books and atlases (39, 59, 64, 65, 73, 74, 84, 104) and with the previous studies (22, 30, 69, 105) that relate the coronal suture with the precentral sulcus in the brain surface and with the foramen of Monro along its coronal level (1, 26, 44, 46, 59, 73, 76, 104).

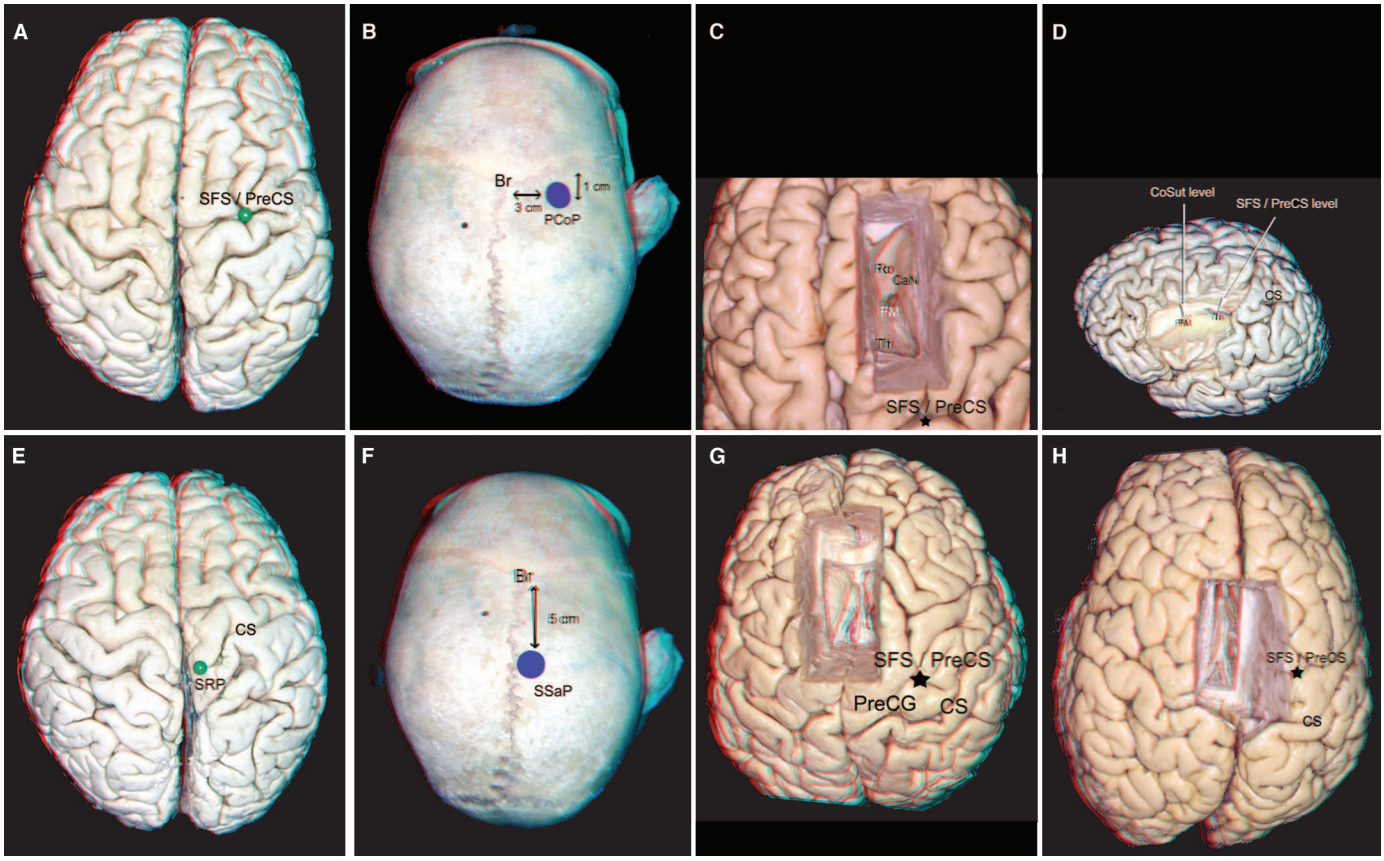

FIGURE 6. *Superior frontal and central key points.* A, *the superior frontal and precentral sulci meeting point (SFS/precentral sulcus) characterizes an important sulcal key point that delineates the anterior aspect of the precentral gyrus at the hand motor activation area level (7), thus constituting the posterior limit of the SFS microsurgical opening.* B, *the SFS/precentral sulcus is located underneath the cranial site situated 1 cm posterior to the coronal suture and 3 cm lateral to the sagittal suture (*PCoP*). These numbers correspond to safe measures because they still tend to dispose this cranial site anterior to the actual SFS/precentral sulcus level.* C *and* D, *whereas the coronal suture radial coronal plane is at the level of the foramen of Monro (*FM*), the SFS/precentral sulcus radial coronal plane is related with the floor of the lateral ventricle body and thus with the superior surface of the thalamus.* E, *the SRP corresponds to the CS and IHF intersection, and is located underneath the cranial site (*F*) 5 cm posterior to the bregma.* G, *SFS transsulcal and the midline transcallosal approach done just anterior to the SFS/precentral sulcus lead to the body of the ventricle.* H, *transcallosal approach done posterior to the SFS/precentral sulcus, thus retracting the precentral gyrus, will be too posterior and lead to the subsplenial pineal region posterior to the junction of both fornices crura.* Br, *Bregma;* CaN, *caudade nucleus;* CoSut, *coronal suture;* CS, *central sulcus;* FM, *foramen of Monro;* PCoP, *posterior coronal point, over SFS/PreCS;* PreCG, *precentral gyrus;* Ro, *rostrum of callosum;* SFS/PreCS, *superior frontal and precentral sulci meeting point;* SRP, *superior Rolandic point;* SSaP, *superior sagital point, over SRP;* Th, *thalamus.*

Superior Rolandic Point

The CS superior extremity is located in the medial surface of each cerebral hemisphere, and its projection on the cerebral hemisphere superior margin, which corresponds approximately to the intersection of the CS with the IHF superior margin, is referred to here by the usual term, SRP (83) (*Fig. 6*).

Analysis of the SRP cranial relationships corroborates the position of the SRP as roughly 5 cm behind the bregma,

with a predominant anterior distribution of up to 1 cm relative to this point (*Table 3*). These findings are in accordance with the classical studies of the 19th century. In his original studies of cranial–encephalic topographic anatomy, Broca investigated 11 adult male cadavers in 1861 and described the SRP as situated in the midline between 40 and 56 mm posterior to the bregma, with an average value of 47 to 48 mm (10, 11). Championniere reported this distance as 5 cm, and around the same time, Poirier (84) described the SRP as located 2 cm posterior to the nasioninian curvature midpoint, as mentioned by Testut and Jacob (84), Passet (55) found it to be 53.4 mm (range, 34–74 mm) posterior to the bregma, Horsley (34) found it to be between 45 and 55 mm, and more recently, Lang (43) found it to be 46.7 mm (range, 36–59 mm) and Ebeling et al. (22) found it to be 46 mm (range, 36–57 mm).

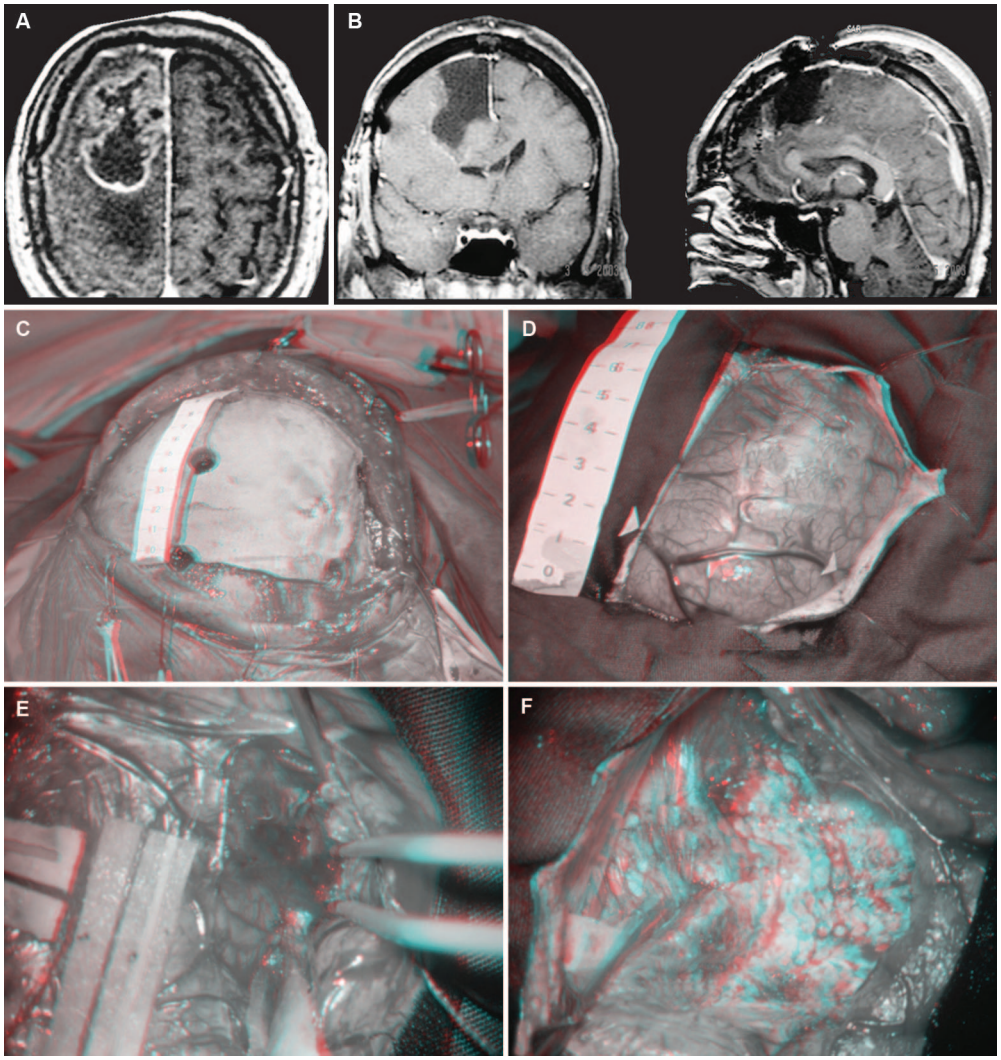

FIGURE 7. *Frontal craniotomy for superior frontal gyrus exposure and tumor removal. Pre-*(A) *and postoperative* (B) *MRI scans pertinent to a right superior frontal gyrus glioblastoma multiform removal with preservation of the cingulate and of the middle frontal gyri in a 49-year-old-male.* C, *right frontal craniotomy placement predominantly anterior to the CoSut, with the patient in the supine position. The craniotomy extends only 2 cm posterior to the CoSut to be anterior to the SFS and precentral sulcus meeting point (SFS/precentral sulcus), which lies underneath the cranial area located 2 cm behind the coronal suture and 3 cm lateral to the sagittal suture.* D, *exposure of the superior and middle frontal gyri anterior to the SFS/precentralsulcus.* E, *opening of the deep SFS, which indicates no tumor infiltration of the middle frontal gyrus.* F, en bloc *removal of the superior frontal gyrus with its enclosed glioblastoma, with preservation of the CiG over the CC.* CC, *corpus callosum;* CiG, *cingulate gyrus;* CoSut, *coronal suture;* MFG, *middle frontal gyrus;* PreCS, *precentral sulcus;* SFG, *superior frontal gyrus;* SFS/PreCS, *superior frontal and precentral sulci meeting point;* SFS, *superior frontal sulcus.*

Superior Frontal and Central Craniotomies

The SFS and the precentral sulcus meeting point (SFS/precentral sulcus) is a reliable key point to be related with frontal and anterior ventricular lesions and to orient and limit transsulcal, transgyral, and interhemispheric frontal approaches (*Figs. 7-10*).

In the cortical surface, the SFS/precentral sulcus lies immediately anterior to the hand motor activation area (7, 105). Regarding its deep relationships, it is particularly related to the floor of the lateral ventricle, which is constituted by the superior thalamic surface. Its correspondent cranial site, which is given by a 2-cm area around the cranial point located 1 cm posterior to the coronal suture and 3 cm lateral to the sagittal suture, can be particularly useful for the proper positioning of craniotomies for frontal and anterior ventricular lesions, which should then be predominantly anterior to the coronal suture for interhemispheric anterior ventricular approaches, as already proposed by other authors (1, 26, 44, 76, 99). Anterior to the coronal suture, the interhemispheric approaches also have the benefit of dealing with fewer bridging veins (64). For interhemispheric anterior transcallosal approaches, the frontal mesial retraction up to the SFS/precentral sulcus level avoids retraction of the paracentral lobule and the callosal section posterior to the paracentral lobule level,

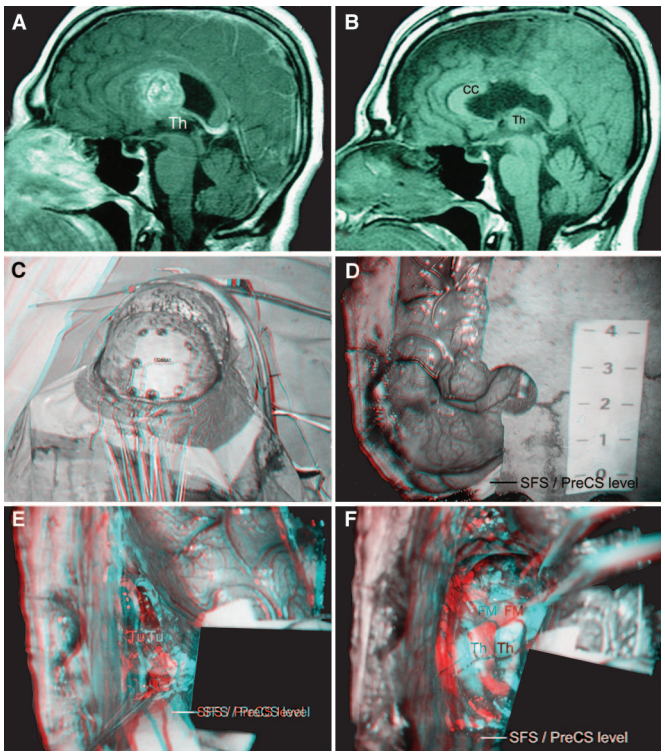

FIGURE 8. *Frontal craniotomy for interhemispheric anterior transcallosal approach and intraventricular tumor removal. Pre-*(A) *and postoperative* (B) *MRI scans of a 51-year-old man with a subependymoma occupying the body and the anterior horn of the right lateral ventricle.* C *and* D, *right frontal craniotomy extending only 3 cm posterior to the coronal suture* (CoSut) *to permit the interhemispheric retraction described below, with patient in the supine position.* E, *exposure of the tumor in the ventricular body after the opening of the corpus callosum with the aid of interhemispheric retraction of the frontal lobe done just anterior to the SFS and precentral sulcus meeting point level (SFS/precentral sulcus)* (F), *which corresponds to the level of the floor of the body of the ventricle given by the superior surface of the thalamus* (Th) *as seen after the tumor removal. The foramen of Monro* (FM) *is at the coronal suture level.* CC, *corpus callosum;* CoSut, *coronal suture;* FM, *foramen of Monro;* preCS, *precentral sulcus;* SFS/PreCS, *superior frontal and precentral sulci meeting point;* Th, *thalamus;* Tu, *tumor.*

which can occasionally cause disconnection syndromes (6), and which also carries the risk of leading into the quadrigeminal cistern, posterior to the ventricular body (*Fig. 6*).

Frontal craniotomies for the mesial exposure of the anterior aspects of the cingulate gyrus and the corpus callosum, including the most common site of pericallosal aneurysms, may require craniotomies with further anterior extensions.

Central craniotomies for the exposure of the precentral and postcentral gyri, the mesial paracentral lobule, and the cingulate gyrus and corpus callosum parts that are inferior to the paracentral lobule should be based on the SFS/precentral sulcus key point and also on the SRP, which lies underneath the bony area located approximately 5 cm behind the bregma. These craniotomies should be predominantly posterior to the coronal suture (*Fig. 10*).

Parietal Key Points

The Intraparietal and Postcentral Sulcus Meeting Point

The concept of IPS and its relationships with the postcentral sulcus vary in the literature; the former is usually constituted by a slightly oblique or longitudinal parietal segment that curves anteriorly, usually becoming continuous with the more inferior part of the postcentral sulcus (24, 80).

In the 19th century, Broca described the IPS separately from the inferior aspect of the postcentral sulcus (11); more recently, Duvernoy (19) considered the lower aspect of the postcentral sulcus as the anterior ascending segment of the IPS, with the postcentral sulcus itself being constituted only by its more superior segment. Ono et al. (54), studying the brain sulci through a more microsurgically oriented point of view, considered them separately (as did Broca), with the IPS being characterized by an usually (almost parallel to the IHF) continuous or interrupted sulcus separating the superior from the inferior parietal lobules. Whereas the superior parietal lobule merges and is continuous with the precuneus in the mesial surface, the inferior parietal lobule is composed by the SMG and AG, usually separated by the ISJ (89), which can be an inferior branch of the IPS, a superior distal branch of the STS, or both.

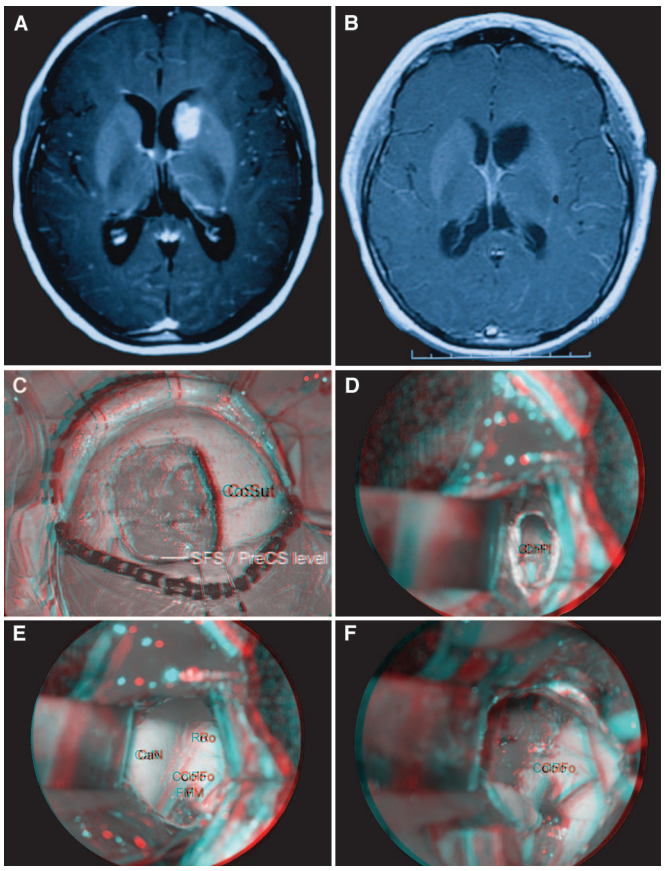

FIGURE 9. *Frontal craniotomy for interhemispheric anterior transcallosal approach and caudate nucleus tumor removal. Pre-*(A) *and postoperative* (B) *MRI scans of a 38-year-old woman with a breast metastasis at the left caudate nucleus head, which increased despite radiosurgery treatment.* C, *patient in the supine position and left frontal craniotomy with posterior extension of only 3 cm posterior to the CoSut, permitting an interhemispheric frontal retraction just anterior to the SFS/precentral sulcus level* (D), *which is related to the level of the lateral ventricle floor given by the choroid plexus* (ChPl) *overlying the superior surface of the thalamus as seen after the corpus callosum opening.* E, *operative view of the left anterior horn after changing the microscope angle view, with the head of the caudate nucleus* (CaN) *constituting its lateral wall, the column of the fornix* (ColFo) *delineating the anterior border of the foramen of Monro* (FM), *and the callosum rostrum* (Ro) *as its floor.* F, *operative view after the removal of the caudate nucleus head with its enclosed metastasis.* CaN, *caudade nucleus;* ChPl, *choroid plexus;* ColFo, *column of fornix;* CoSut, *coronal suture;* FM, *foramen of Monro;* Ro, *rostrum of callosum;* SFS/PreCS, *superior frontal and precentral sulci meeting point.*

Anteriorly, the IPS is, thus, particularly related with the postcentral sulcus, and posteriorly it is usually continuous with the intraoccipital sulcus (19, 50), which is also called the transverse occipital sulcus (54, 96) and the superior occipital sulcus (84), and which separates the more evident superior from the middle occipital gyrus (50, 84). The lateral occipital sulcus (54, 96) or inferior occipital sulcus (84) separates the middle and the inferior occipital gyri, and the lunate sulcus, when present, lies anterior to the occipital pole (54, 96).

According to previous studies (24, 54, 80) and to our findings, the IPS can be characterized morphologically as continuous (83%) or noncontinuous (17%) with the postcentral sulcus, and it can have a longitudinal (89%) or a transverse (11%) disposal relative to the IHF.

The point referred to in our study as the IPS/postcentral sulcus meeting point (IPS/postcentral sulcus) corresponds with the connection or transition point between these two sulci, or to the postcentral sulcus point more particularly related to the most anterior aspect of the IPS level when these two sulci are not continuous. The IPS/postcentral sulcus constitutes an important neurosurgical key point because 1) it is an evident point that delineates posteriorly the postCG, 2) it can be used as a safe starting point for the microsurgical opening of these sulci, and 3) it has a deep relationship with the ventricular trigone, as also shown by Harkey et al. (32) (*Fig. 11*). Despite the sulcal and gyral variability of the parietal opercular region described by Ebeling and Steinmetz (24) and Steinmetz et al. (80), these authors also concluded that the junction between the postcentral sulcus and the IPS is indeed a prominent sulcal landmark for radiological and surgical purposes (24).

The IPS/postcentral sulcus key point is a midparietal point, and our findings of its distance from the midline (mean distance from the IHF, 3.96 $\pm$ 0.67 cm) are similar to those obtained by Harkey et al. (32) (mean, 42 mm; range, 35–50 mm).

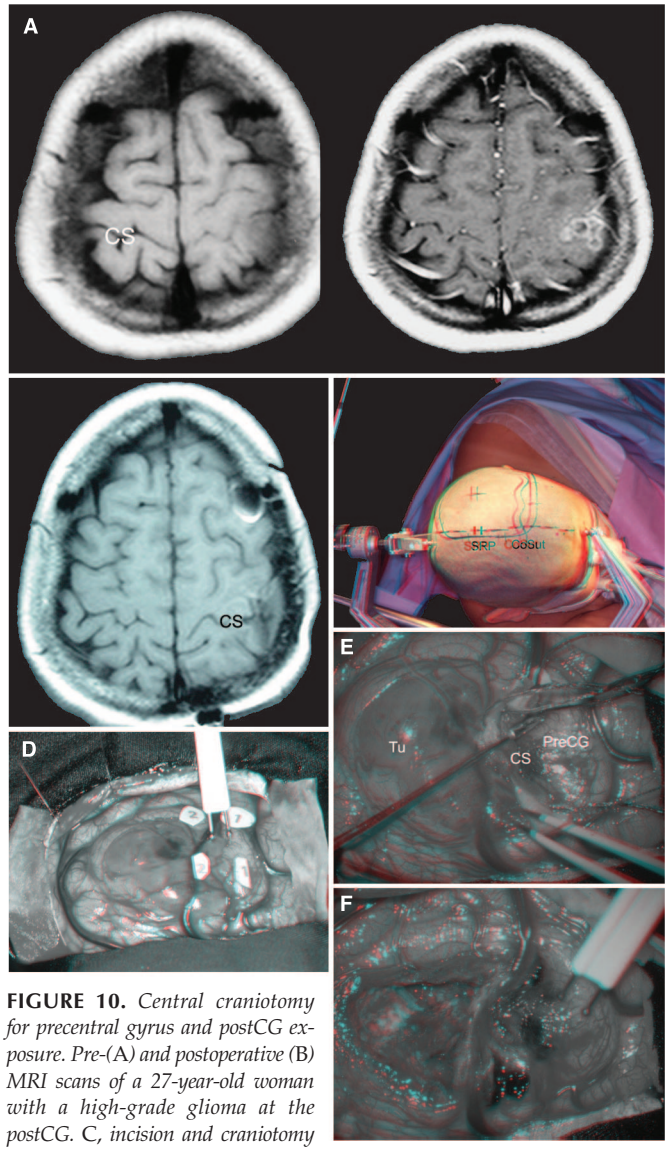

FIGURE 10. *Central craniotomy for precentral gyrus and postCG exposure. Pre-*(A) *and postoperative* (B) *MRI scans of a 27-year-old woman with a high-grade glioma at the postCG.* C, *incision and craniotomy site with patient in lateral position and considering the position of the SRP 5 cm posterior to the CoSut.* D, *cortical exposure and motor mapping for identification of the precentral gyrus (1) and the postCG (2) harboring the tumor* (Tu). E, *opening of the CS separating the Tu from the precentral gyrus.* F, *operative view and motor stimulation after the tumor removal.* CoSut, *coronal suture;* CS, *central sulcus;* PreCG, *precentral gyrus;* SRP, *superior Rolandic point;* Tu, *tumor.*

Analysis of the cranial relationships of the IPS/postcentral sulcus key point shows that the cranial point examined initially, 5 cm anterior to the lambdoid and 4 cm lateral to the midline, was found to be too posterior to the postcentral sulcus (1.31 ± 0.67 cm; 90th percentile, 2.28 cm) and slightly medial to the IPS (0.42 ± 0.52 cm; 90th percentile, 1.00 cm), requiring the correction of its positioning to an interval of less than 2 cm from the IPS/postcentral sulcus. Because advancement of the proposed cranial point theoretically increases its medial distance from the IPS, given the usual predominant anterior and inferior direction of the IPS, its correction should be done in both directions. Thus, the IPS/postcentral sulcus key point should then be located underneath the cranial point 6 cm anterior to the λ and 5 cm lateral to the sagittal suture (*Fig. 11*).

Regarding its deep relationship with the ventricular cavity, the IPS/postcentral sulcus meeting point that actually corresponds to the point of the postcentral sulcus most particularly related with the IPS anterior extremity level was found to be particularly related with the ventricular atrium along a 30- degree posteriorly oblique radial approach in 95% of the specimen.

The EOF Medial Point

The EOF (10, 11), which corresponds to the extension of the medial POS into the brain convexity, was evident in this study as a deep transversal sulcus on the medial side of the superolateral face of each hemisphere (EOF average length, 3.95 ± 0.64 cm). Its most medial point (EOF/POS), which corresponds to the most superior point of the POS, constitutes an useful surgical landmark because it defines the POS position and, thus, the posterior aspect of the precuneus along the IHF (average distance between the EOF/POS and the postcentral sulcus, equivalent to the longitudinal extension of the precuneus along the IHF: 3.95 ± 0.64 cm) (*Fig. 11*).

As shown by Broca (11), the EOF and EOF/POS are very closely related with the λ. Our EOF/POS cranial relationship findings show that this sulcal key point, which indicates the POS emergence in the IHF, lies underneath each paramedian area corresponding to the angle between the sagittal and lambdoid suture (La/Sa) in each cranial side, within an interval range of less than 2 cm (average distance of EOF/POS to La/Sa: anterior, 0.23 ± 0.39 cm; 90th percentile, 0.94 cm).

Euryon

Given its palpatory evidence, the craniometric point that corresponds to the center of the parietal tuberosity (i.e., the euryon) (9, 10, 59) was studied regarding its own characteristics and its related cortical area (*Fig. 11*).

Regarding its own topography, the euryon was found to be closely related to the superior temporal line (immediately superior to the superior temporal line, 91%; on the superior temporal line, 9%), and with a vertical line that passes through the posterior aspect of the mastoid tip and through the squamous suture and parietomastoid suture meeting point (parietomastoid suture/squamous suture) (average distance of the euryon from this vertical line: anteriorly, 0.23 ± 0.75 cm; average vertical distance of the euryon from the parietomastoid suture/squamous suture: 6.48 ± 0.79 cm).

Relative to the cortical surface, the euryon was found, in all cases, to be over the superior aspect of the SMG and, more frequently, over its posterior half, and thus superior to

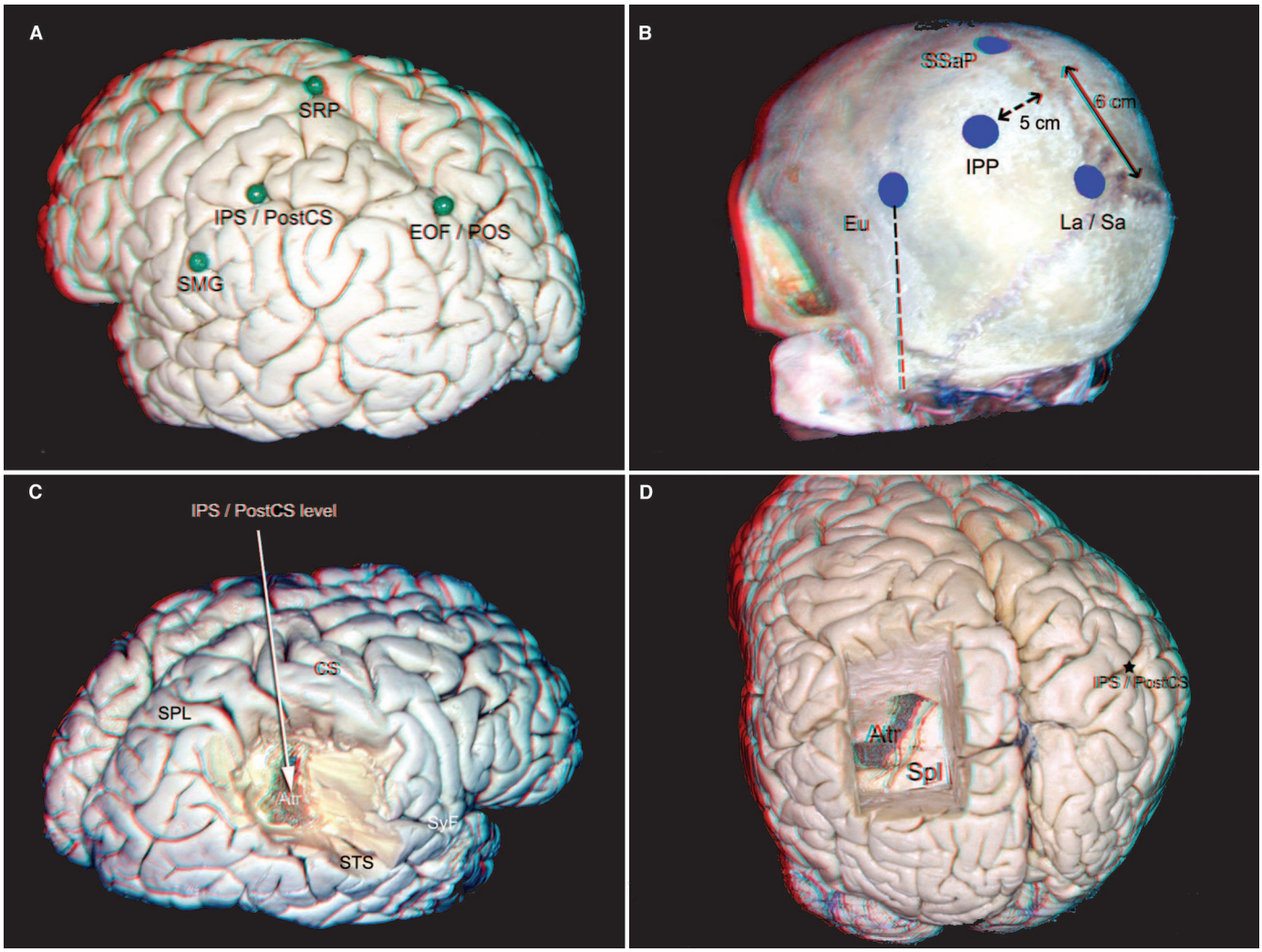

FIGURE 11. *Parietal key points.* A, *the parietal sulci and gyri topography can be estimated through the identification of the SRP that indicates the position of the CS superior aspect; the IPS and postcentral sulcus meeting or transitional point (IPS/postcentral sulcus), which should be identified as the postcentral sulcus point most particularly related with the IPS anterior extremity level; the SMG's most prominent aspect; and the medial extremity of the external occipital fissure (*EOFm*) that corresponds to the most superior extremity of the POS.* B, *the SRP is located underneath the cranial area 5 cm posterior to the bregma (superior sagittal point). The IPS/postcentral sulcus is located underneath the cranial area located 6 cm anterior to the λ and 5 cm lateral to the sagittal suture. The SMG is located underneath the euryon that corresponds to the most prominent point of the parietal tuberosity, roughly along a vertical line originating at the posterior aspect of the mastoid tip and passing through the parietomastoid suture and squamous suture meeting point. The EOF/POS is located underneath the cranial area that corresponds to the angle between the lambdoid and the sagittal suture (La/Sa).* C *and* D, *the IPS/postcentral sulcus key point enables the identification of the IPS and postcentral sulcus and is radially particularly related with the atrium (*Atr*) at its depth. It is important to stress that the IPS opening posterior to the IPS/postcentral sulcus can enlarge the exposure of the ventricular Atr but progressively runs away from this cavity; the key point for the Atr approach is the IPS/postCG itself.* Atr, *atrium of lateral ventricle;* EOF/POS, *external occipital fissure most medial point, equivalent to the most superior point of the parieto-occipital sulcus;* Eu, *Euryon, over SMG;* IPP, *intraparietal point, over IPS/PostCS;* IPS/PostCS, *intraparietal and poscentral sulci meeting point;* La/Sa, *angle between the lambdoid and the sagital sutures, over EOFm;* SMG, *supramarginal gyrus;* Spl, *splenium of corpus callosum;* SPL, *superior parietal lobule;* SRP, *superior rolandic point;* SSaP, *superior sagital point, over SRP;* STS, *superior temporal sulcus;* SyF, *sylvian fissure.*

the posterior sylvian point (average distance, 2.60 ± 0.66 cm), posterior to the postcentral sulcus (average distance, 2.12 ± 0.72 cm), lateral to the IPS (average distance, 2.00 ± 0.84 cm), and anterior to the ISJ (89), which separates the SMG from the AG (average distance, 1.56 ± 0.78 cm).

In the dominant hemisphere, the cortical area underneath the euryon is very much related with the parietal speech zone, which, although relatively spread (53), has its core located approximately 1 to 4 cm above the sylvian fissure and 2 to 4 cm behind the postcentral sulcus (31, 63).

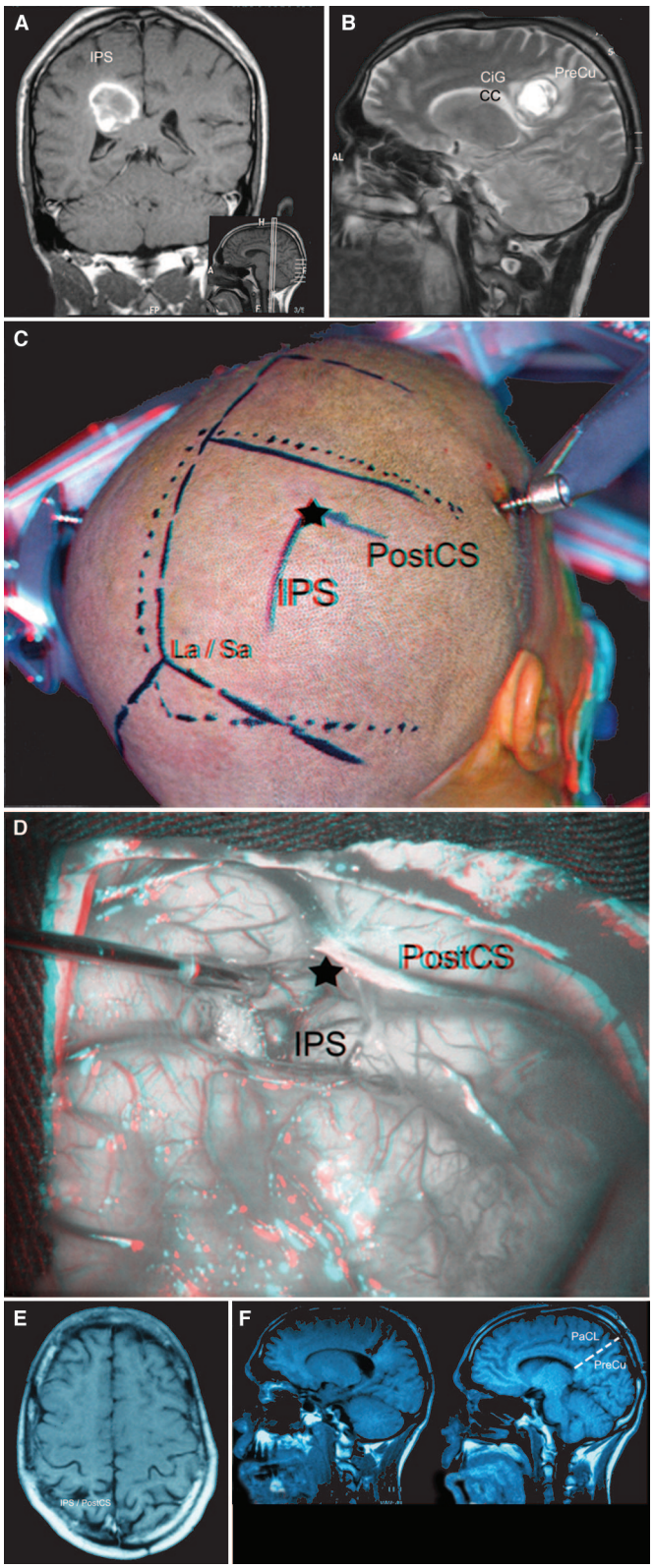

FIGURE 12. *Parietal craniotomy for IPS exposure and dissection towards the atrium.* A *and* B, *preoperative MRI scans of a 28-year-old man with a cavernoma located below the depth of the most anterior part of the right IPS, just above the roof of the right ventricular atrium, mostly at the base of the precuneus* (preCu) *and at the CiG.* C, *incision* (dotted lines) *for a right parietal craniotomy, with patient in semisitting position. Note the position of the IPS and postcentral sulcus sulci and their meeting point (★), which is situated underneath the cranial area located 6 cm anterior to the λ and 5 cm lateral to the sagittal suture, and of the medial point of the EOF, which corresponds to the most superior point of the POS and which is located underneath the cranial area of the angle between the lambdoid and the sagittal sutures (La/Sa).* D, *exposure and opening of the most anterior aspect of the IPS, just posterior to the postcentral sulcus, which radially leads towards the atrium and, in this case, to the cavernoma.* E, *postoperative axial MRI scan indicating the transsulcal entrance through the IPS and postcentral sulcus meeting point area (IPS/postcentral sulcus). Note the posteriorly located connection arm that interrupts the IPS and that is evident both in the previous operative view and in this MRI image.* F, *postoperative MRI sagittal images showing the operative track* (dotted lines) *originating at the IPS/postcentral sulcus and radially oriented towards the atrium, located along the most anterior aspect of the preCu, just posterior to the marginal ascending ramus of the cingulate sulcus, which posteriorly delineates the PaCL.* CC, *corpus callosum;* CiG, *cingulate gyrus;* IPS/PostCS, *intraparietal and poscentral sulci meeting point (★);* IPS, *intraparietal sulcus;* La/Sa, *angle between the lambdoid and the sagittal sutures, over the external occipital fissure most medial point which is equivalent to the most superior point of the parieto-occipital sulcus (EOF/POS);* PaCL, *paracentral lobule;* PostCS, *postcentral sulcus;* PreCu, *precuneus.*

Parietal Craniotomies

Parietal craniotomies should have, as their main landmarks, 1) the IPS and the postcentral sulcus transition point (IPS/postcentral sulcus), which should be understood as the point of the postcentral sulcus most particularly related to the anterior extremity of the IPS, and which is located under the cranial site 6 cm anterior to the lambdoid and 5 cm lateral to the sagittal suture; 2) the EOF medial point (EOF/POS), which corresponds to the emergence of the POS on the superior aspect of the IHF, and which lies just anterior to the La; and 3) the Eu, which corresponds to the center of the parietal tuberosity, and which is located over the SMG (*Figs. 12–14*).

The position of the λ in adults can be estimated through its distances from the other midline craniometric points (25.0 ± 1 cm posterior to the nasion; 13 ± 1 cm posterior to the bregma; 3 ± 1 cm anterior to the opisthocranion) (*Fig. 2*). The close relationships that were found between the euryon and the vertical line originating at the mastoid tip posterior aspect and between the euryon and the superior temporal line can, respectively, help its palpatory recognition and its intraoperative localization.

The exposure of the superior parietal lobule also requires the knowledge that the SRP lies underneath the cranial point located 5 cm posterior to the bregma; together, the SRP and the EOF/POS define the extension of the postCG and the precuneus along the midline.

The exposure of the inferior parietal lobule can be particularly aided by exposure of the visually evident distal part of the sylvian fissure because its identification corroborates the identification of the basal aspect of the SMG and also because of its connection with the superior temporal gyrus that encircles the distal segment of the sylvian fissure (54, 64). For its

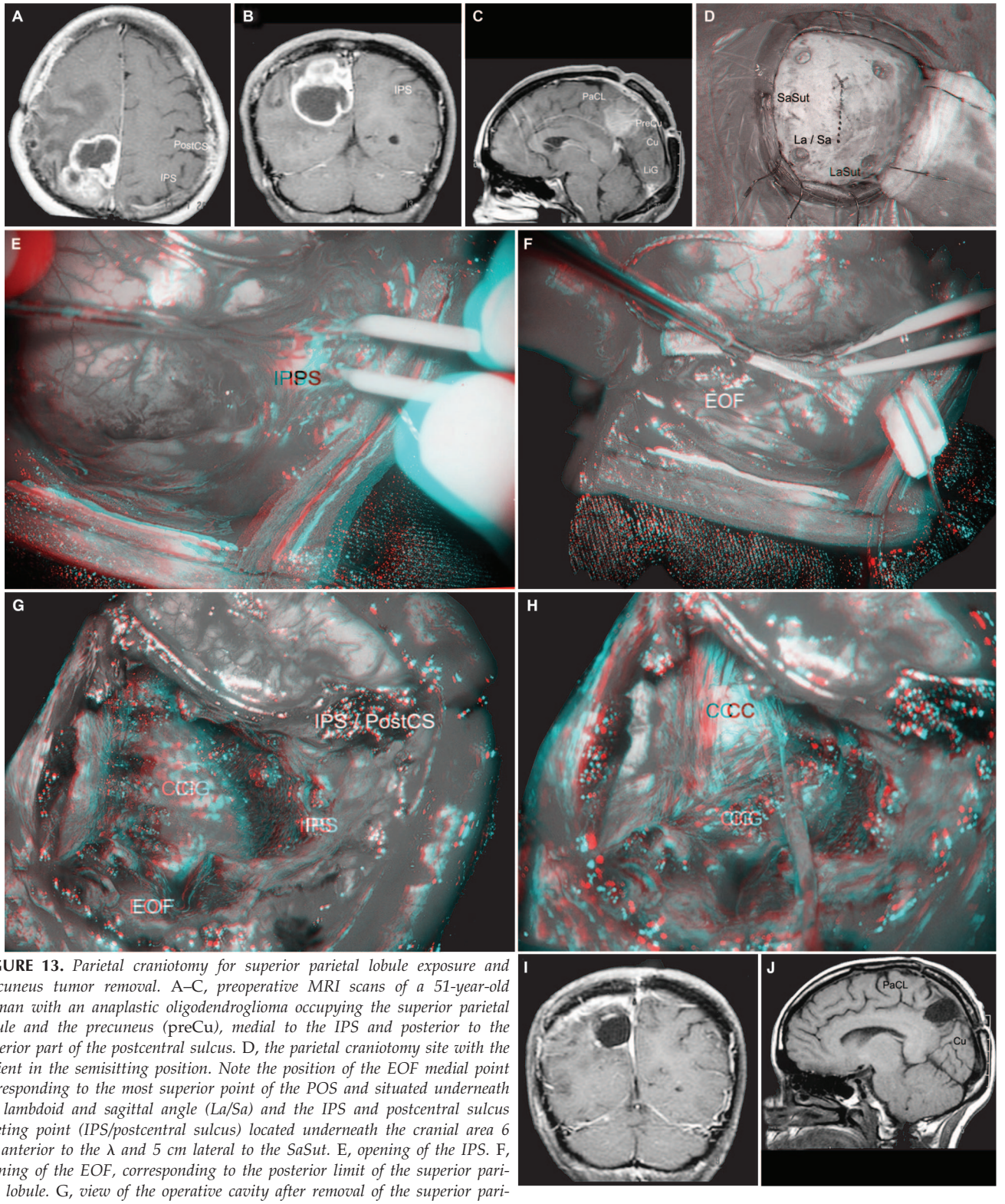

FIGURE 13. *Parietal craniotomy for superior parietal lobule exposure and precuneus tumor removal.* A–C, *preoperative MRI scans of a 51-year-old woman with an anaplastic oligodendroglioma occupying the superior parietal lobule and the precuneus (*preCu*), medial to the IPS and posterior to the superior part of the postcentral sulcus.* D, *the parietal craniotomy site with the patient in the semisitting position. Note the position of the EOF medial point corresponding to the most superior point of the POS and situated underneath the lambdoid and sagittal angle (La/Sa) and the IPS and postcentral sulcus meeting point (IPS/postcentral sulcus) located underneath the cranial area 6 cm anterior to the λ and 5 cm lateral to the SaSut.* E, *opening of the IPS.* F, *opening of the EOF, corresponding to the posterior limit of the superior parietal lobule.* G, *view of the operative cavity after removal of the superior parietal lobule, medially contiguous with the precuneus and the enclosed tumor, and superior to the CiG that was preserved.* H, *view of the corpus callosum with the retraction of the CiG.* I *and* J, *postoperative MRI images indicating the postoperative cavity that corresponds to the superior parietal lobule and the contiguous precuneus that enclosed the tumor.* CC, *corpus callosum;* CiG, *cingulate gyrus;* Cu, *cuneus;* EOF, *external occipital fissure;* IPS/PostCS, *intraparietal and postcentral sulci meeting point;* IPS, *intraparietal sulcus;* La/Sa, *angle between the lambdoid and the sagittal sutures, over the external occipital fissure most medial point which is equivalent to the most superior point of the parieto-occipital sulcus (EOF/POS);* LaSut, *lambdoid suture;* LiG, *lingual gyrus;* PaCL, *paracentral lobule;* PostCS, *postcentral sulcus;* PreCu, *precuneus;* SaSut, *sagittal suture.*

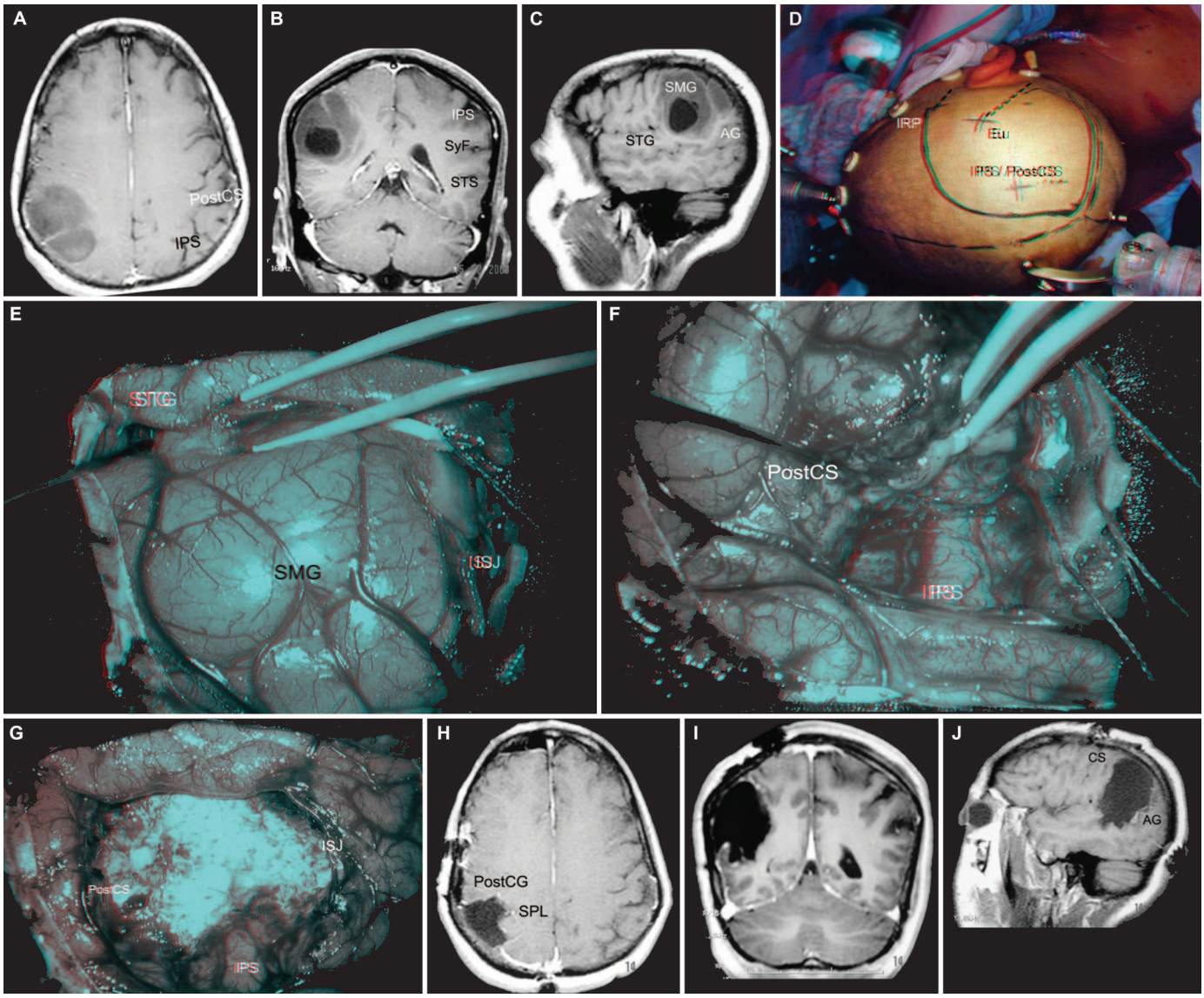

FIGURE 14. *Parietal craniotomy for inferior parietal lobule exposure andSMG tumor removal.* A–C, *preoperative MRI scans of a 42-year-old woman with a low-grade glioma (Grade II astrocytoma) within the SMG of the right inferior parietal lobule. The tumor lies lateral to the IPS, posterior to the postcentral sulcus, and superior to the flat distal part of the sylvian fissure that constitutes the temporal plane, and seems not to infiltrate the AG that constitutes the posterior part of the inferior parietal lobule.* D, *incision for right parietal craniotomy, with patient in lateral position. Note the position of 1) the Eu, which constitutes the most prominent point of the parietal tuberosity, is situated along a vertical line originated at the posterior aspect of the mastoid tip, and overlies the SMG; 2) the IPS and postcentral sulcus meeting point (IPS/PostCS) underneath the cranial area located 6 cm anterior to the λ and 5 cmlateral to the sagittal suture, which will lead to both of these sulci that partially encircle the tumor; and 3) the IRP, which is located underneath the cranial area located at the intersection of the squamous suture with a vertical line originating at the preauricular depression, enabling the exposure of the most posterior part of the sylvian fissure.* E, *operative exposure of the SMG area, which harbors the tumor, with the bipolar forceps indicating the connection arm between the SMG and the STG, and with an SMG posterior sulcus already opened and filled with cottonoids, constituting the ISJ, which separates the SMG from the AG.* F, *opening of the IPS.* G, *operative view after the SMG with the enclosed tumor removal. The ISJ was continuous with the posterior aspect of IPS, and the inferior part of the postcentral sulcus was dissected and opened as an anterior and inferior continuous extension of the IPS.* H to J, *postoperative MRI images showing the selective removal of the SMG inferior to the superior parietal lobule (SPL), posterior to the postCG, and anterior to the AG.* AG, *angular gyrus;* CS, *central sulcus;* Eu, *Euryon, over SMG;* IPS/PostCS, *intraparietal and postcentral sulci meeting point;* IRP, *inferior rolandic point;* ISJ, *intermediary sulcus of Jensen, between SMG and AG;* PostCG, *postcentral gyrus;* PostCS, *postcentral sulcus;* PS, *intraparietal sulcus;* SMG, *supramarginal gyrus;* SPL, *superior parietal lobule;* STG, *superior temporal gyrus;* STS, *superior temporal sulcus;* SyF, *sylvian fissure.*

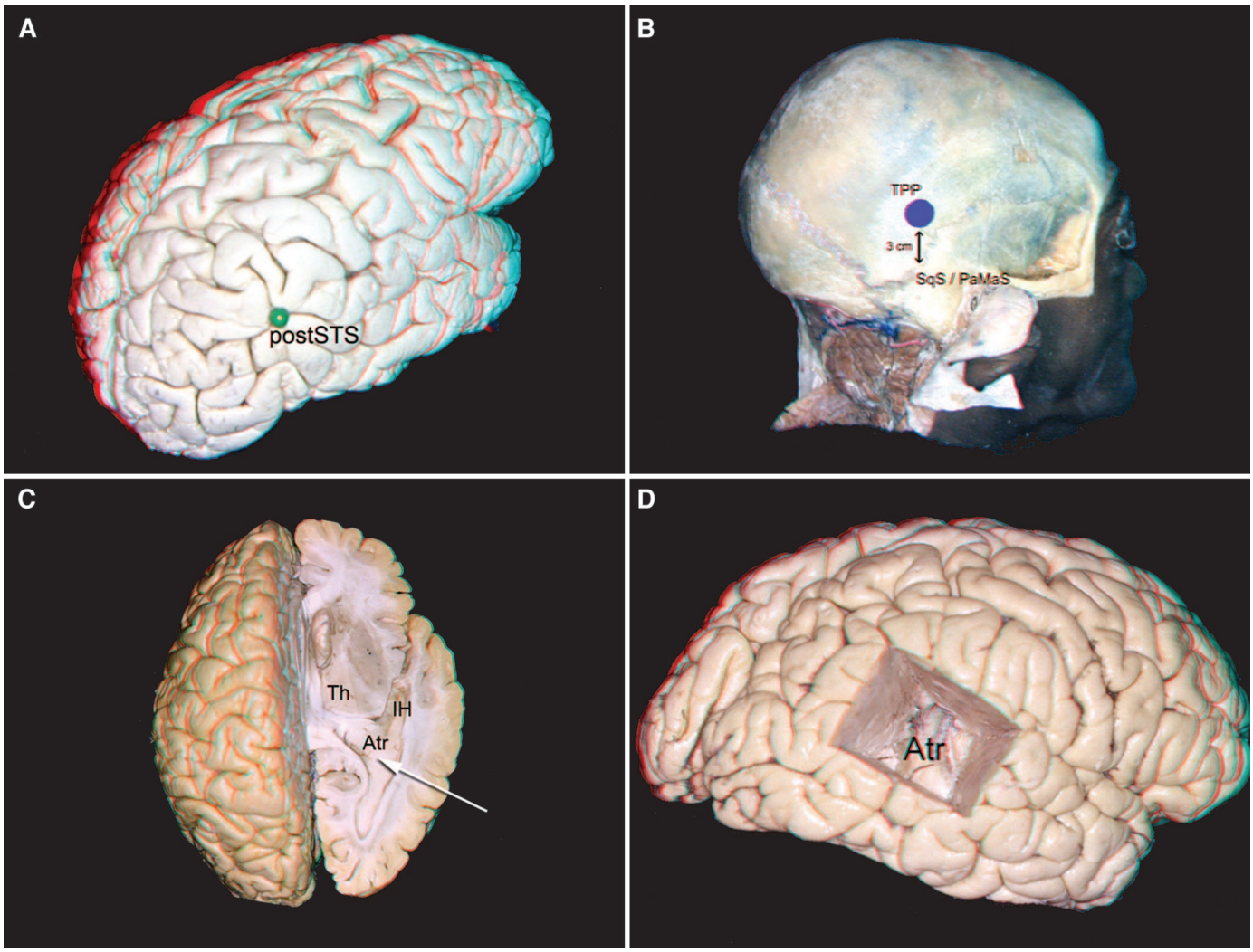

FIGURE 15. *Posterior temporal key point.* A, *the superior temporal sulcus constitutes an appropriate microsurgical corridor to the ventricular inferior horn* (IH) *and atrium* (Atr), *and its posterior segment before its usual distal bifurcation* (postSTS) *is located posterior and inferior to the distal aspect of the sylvian fissure. Thus, it is posterior to the insula, the posterior limb of the internal capsule, and the thalamus.* B, *the postSTSlies underneath the cranial area located 3 cm above the evident Sqs/Pa.* C *and* D, *a radially oriented, anteriorly oriented approach through the opening of the postSTS leads to the Atr.* Atr, *atrium of lateral ventricle;* IH, *inferior horn;* PaMaSut/SqSut, *parietomastoid and squamous and parietomastoid sutures meeting point;* postSTS, *superior temporal sulcus posterior segment distal extremity;* SqS/PaMaSut, *squamous sutures meeting point;* Th, *thalamus;* TPP, *temporoparietal point.*

exposure, it is helpful to consider our findings showing that the posterior sylvian point lies 2 to 3 cm inferior to the Eu.

On the cortical surface, the most prominent point of the SMG that lies underneath the euryon was found to be located 1.5 to 2.5 cm posterior to the postcentral sulcus and 1.5 to 2.5 cm lateral to the IPS.

Although more frequently interrupted (54), the IPS was found to have an evident continuous segment (average length, 3.19 ± 1.17 cm), which was usually longitudinal in relation to the IHF (89%), and which delineates the superior aspect only of the SMG (56%) and AG (44%). Both the IPS and its frequently continuous postcentral sulcus are often covered by a cortical vein (64).

The depth of the IPS has been studied by Ebeling and Steinmetz (24) (mean, 20 mm; range, 13–26 mm) and by Harkey et al. (32) (mean, 24 mm; range, 20–27 mm) and has been shown to be usually microneurosurgically significant.

For IPS transsulcal approaches to the ventricular cavity, it is important to stress that its closest topographical relationship with the atrium is given particularly by its most anterior part. Because the intersection point of the IPS (or its anterior extension) with the postcentral sulcus (IPS/postcentral sulcus) is coronally posterior to the atrium and related to the splenium (at the level of the splenium, 75%; posterior to the splenium, 25%; average distance from the splenium: posterior, 0.23 ± 0.50 cm), the transsul-

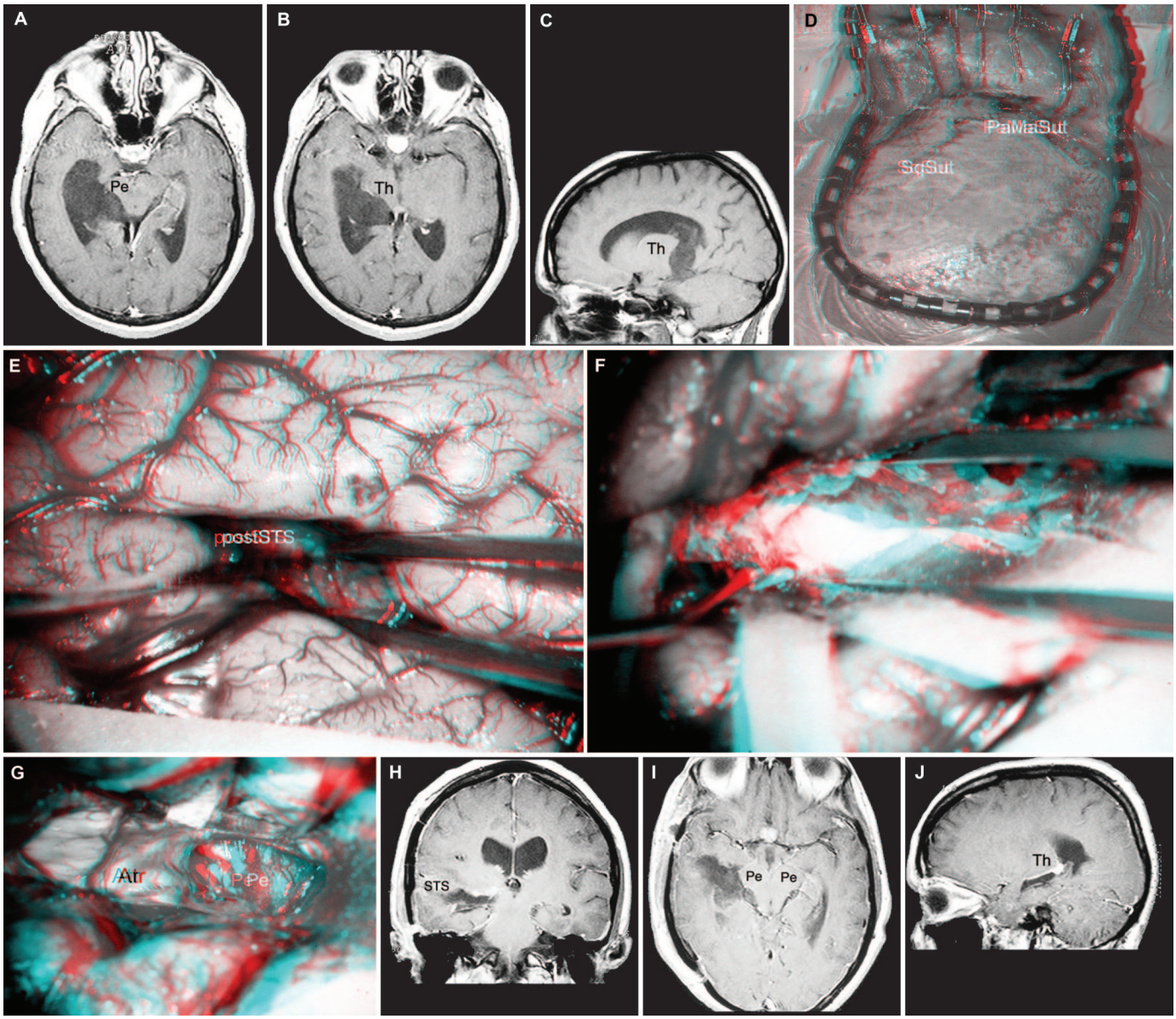

FIGURE 16. *Posterior temporal craniotomy for exposure of the postSTS and right inferior horn and atrium* (Atr) *tumor removal.* A–C, *preoperative MRI scans of a 43-year-old woman with a right intraventricular dermoid tumor occupying the inferior horn and the Atr, and extension to the ambient cistern through an opened choroidal fissure.* D, *operative exposure of the cranial surface, with patient in lateral position, indicating the horizontal parietomastoid suture and the oblique posterior segment of the squamous suture. The postSTS lies underneath the cranial area located 3 cm above the evident meeting point of both sutures.* E, *opening of the postSTS.* F, *exposure of the very white dermoid tumor in the right inferior horn.* G, *operative exposure after tumor removal, indicating the empty right Atr and ambient cistern next to the cerebral peduncle* (Pe) *shown through a widely opened choroidal fissure.* H–J, *postoperative MRI scans indicating the operative track through the STS and right inferior horn, Atr, and ambient cistern free of tumor.* Atr, *atrium of lateral ventricle;* PaMaSut, *parietomastoid suture;* Pe, *cerebral peduncle;* postSTS, *posterior segment of the superior temporal sulcus;* SqSut, *squamous suture;* Th, *thalamus.*

cal approach to the atrium from the IPS/postcentral sulcus was shown to be possible only along a 30- to 45-degree posteriorly oblique radial approach. The IPS opening posterior to the IPS/postcentral sulcus key point enlarges its exposure but runs progressively away from the atrium.

Regarding possible surgical complications attributable to parietal transsulcal and transgyral approaches, in the dominant hemisphere language impairments can be related to the damage of the SMG and AG that lie lateral to the IPS (31, 53, 63), and in the nondominant hemisphere the parietal

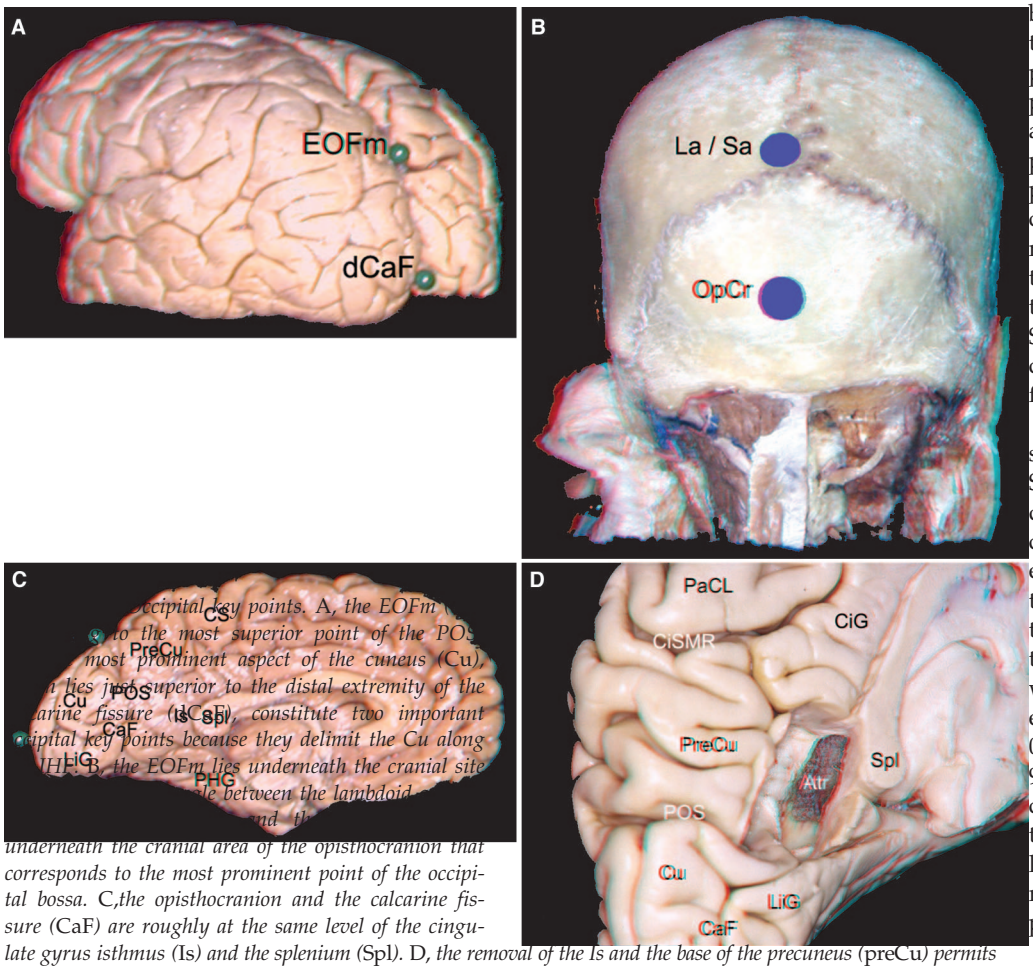

*occipital key points. A, the EOFm (
to the most superior point of the POS
most prominent aspect of the cuneus (Cu),
lies just superior to the distal extremity of the
larine fissure (dCaF), constitute two important
cipital key points because they delimit the Cu along
IH; B, the EOFm lies underneath the cranial site
ole between the lambdoid
nd th
underneath the cranial area of the opisthocranion that corresponds to the most prominent point of the occipital bossa. C,the opisthocranion and the calcarine fissure (CaF) are roughly at the same level of the cingulate gyrus isthmus (Is) and the splenium (Spl). D, the removal of the Is and the base of the precuneus (preCu) permits the lateral exposure of the atrium (Atr) from the occipital interhemispheric approach.* Atr, *atrium;* CaF, *calcarine fissure;* CiG, *cingulate gyrus;* CS, *central sulcus;* Cu, *cuneus;* dCaF, *distal extremity of calcarine fissure;* EOF/POS, *external occipital fissure most medial point, equivalent to the parieto-occipital sulcus most superior point;* Is, *isthmus of cingulate gyrus;* La/Sa, *angle between the lambdoid and the sagital sutures, over EOFm;* LiG, *lingual gyrus;* OpCr, *Opisthocranion, over distal calcarine fissure;* PaCL, *paracentral lobule;* PHG, *parahippocampal gyrus;* POS, *parieto-occipital sulcus;* PreCu, *precuneus;* Spl, *splenium of corpus callosum;* CiSMR, *cingular sulcus marginal ramius.*

damage can cause derangement of complex functions involving somatic as well as psychic elements, which have as a common feature a defective recognition of sensory impressions (neglect, agnosias), and which are especially marked in tasks that require appreciation of spatial relationships (13).

Posterior Temporal Key Point

The Superior Temporal Sulcus Posterior Portion and Posterior Extremity

The superior temporal sulcus constitutes an important microsurgical corridor to the entire inferior horn of the lateral ventricle; through its posterior portion, the ventricular atrium also can be approached (32). According to the present findings, this posterior transtemporal approach can be started through a STS posterior segment that is located posterior and inferior to the posterior sylvian point, along an approximately 45- degree posterior inclined plane. The postSTS studied here can be characterized by a sulcal segment, which may (88%) be continuous or not continuous with the more anterior aspect of the STS, and which usually precedes a common STS distal bifurcation (*Fig. 15*).

The postSTS cranial relationship findings indicate that the STS posterior segment lies underneath the cranial site located 3 cm vertically above the evident meeting point between the parietomastoid suture and the ascending squamous suture posterior aspect (66), within much less than 2 cm of error (average distance, 0.01 ± 0.37 cm inferior to the postSTS; 90th percentile, 0.24 cm). The corresponding cranial point of the postSTS was shown to be located just below the posterior aspect of the superior temporal line in all cases.

This cranial point, which lies over the postSTS, was also studied regarding its position relative to the posterior sylvian point and was shown to be 2 to 3 cm posterior and inferior to the sylvian fissure (average vertical distance, 1.37 ± 0.63 cm; average horizontal distance, 2.00 ± 0.82 cm; average direct distance, 2.35 ± 0.80 cm).

Posterior Temporal Craniotomies

Considering these findings, temporal posterior craniotomies for posterior temporal and inferior parietal cortical exposures and for approaches to the posterior aspect of the inferior horn can be centered at the postSTS, which is situated underneath the cranial site localized 3 cm vertically above the transition point between the horizontal parietomastoid suture and the oblique posterior aspect of the squamous suture (*Fig. 16*).

The concomitant exposure of the distal aspect of the sylvian fissure, located 2 to 3 cm anterior and superior to this cranial point, is helpful in identifying of the sulci and gyri of this region.

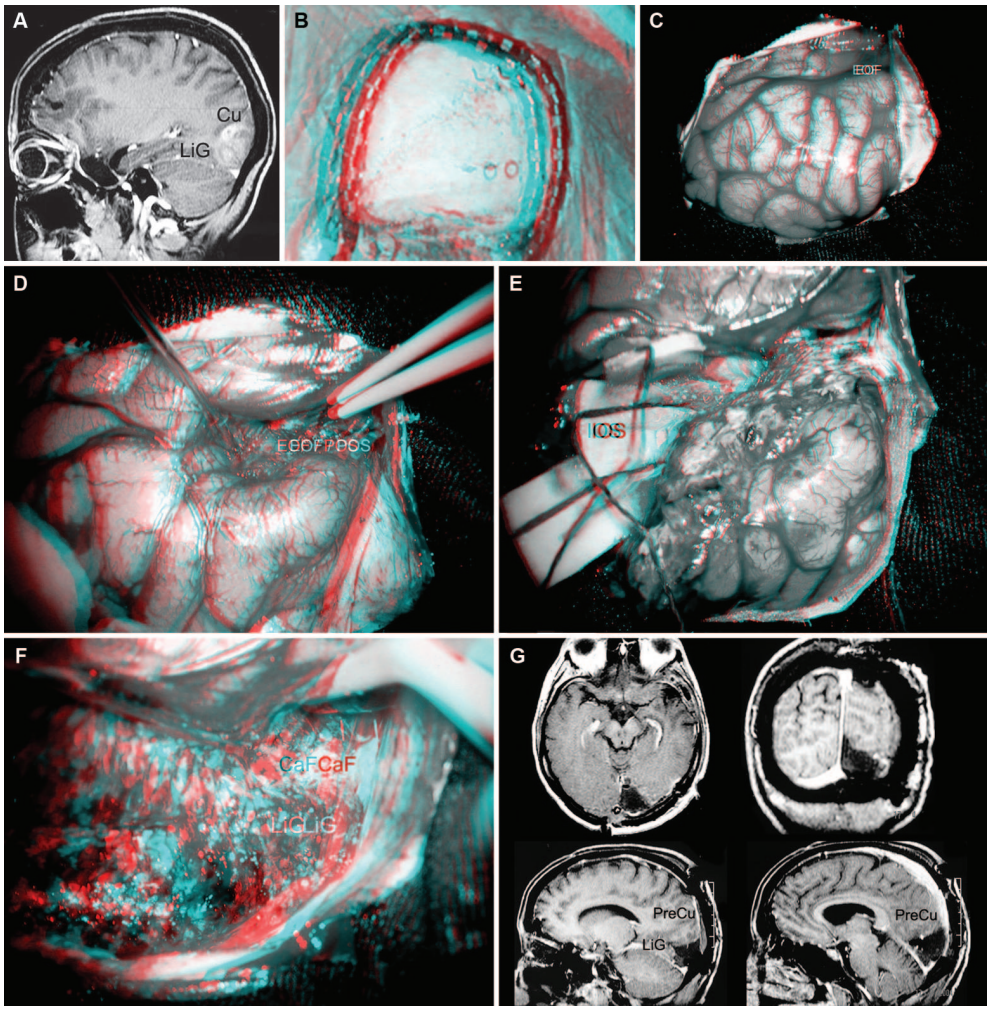

FIGURE 18. *Occipital craniotomy for cuneus* (Cu) *and lingual gyri* (LiG) *exposure and occipital tumor removal.* A, *preoperative MRI scan of a 42-year-old woman with a glioblastoma multiform occupying the left Cu and the posterior part of the LiG.* B, *operative cranial exposure, with the patient in the sitting position, indicating the lambdoid suture* (LaSut), *the lambdoid and sagittal sutures angle (La/Sa) overlying the medial point of the EOF and corresponding to the most superior point of the POS, and the opisthocranion, which corresponds to the most prominent point of the cranial occipital bossa and overlies the most posterior aspect of the Cu and the distal extremity of the calcarine fissure.* C, *operative view of the occipital pole, limited superiorly by the EOF.* D, *opening of the EOF, medially contiguous with the POS (EOF/POS).* E, *opening of the IOS, also called transverse and superior occipital sulcus, which separates the superior occipital gyrus medially from the middle occipital gyrus laterally.* F, *operative view after the removal of the occipital pole, constituted by the superior occipital gyrus and its medially contiguous Cu and posterior part of the LiG. Note the calcarine fissure* (CaF) *above the remnant part of the LiG, with the bipolar uplifting of the base of the precuneus within the empty space left by the Cu removal.* G, *postoperative MRI images showing the above-mentioned removal.* CaF, *calcarine fissure;* Cu, *cuneus;* EOF/POS, *external occipital fissure contiguous with parieto-occipital sulcus;* EOF, *external occipital fissure;* IOS, *interoccipital sulcus, also called superior and transverse occipital sulcus;* L, *lambda, indicating the angle between the lambdoid and the sagittal sutures, over the external occipital fissure medial point that is equivalent to the parieto-occipital sulcus most superior point (EOF/POS);* LiG, *lingual gyrus;* O, *opisthocranion, most prominent occipital point;* PreCu, *precuneus.*

The basal aspect of posterior temporal craniotomies should be immediately superior to the evident parietomastoid suture and the squamous suture transition point mentioned above because this point is related to the superior surfaces of the petrous bone and to the tentorium petrosal attachment (66).

In addition to temporal horn lesions, the postSTS approach is also adequate for nondominant ventricular atrial lesions that extend inferiorly toward the inferior horn and, eventually, to the ambient and quadrigeminal cisterns through the choroidal fissure. Although optic radiation fibers are damaged (21), this approach, when limited, usually does not cause significant visual deficits (35).

Transcerebral posterior temporal approaches should be avoided in the dominant hemisphere because of their possible consequent language impairments (53).

Occipital Key Point

Opisthocranion

The opisthocranion, the craniometric point that corresponds to the most prominent occipital cranial point (10, 11, 59), was evident in all studied specimen (*Fig. 17*). Regarding its cortical relationships, the opisthocranion was shown to be related to the superior aspect of the distal and the calcarine fissure and, thus, with the base of the cuneus, within an error interval significantly less than 2 cm (*Table 5*). The distance of the opisthocranion to the occipital base of approximately 2 cm indicates the height of the lingual gyrus.

Occipital Craniotomies

Occipital craniotomies intended to expose all the medial aspects of the occipital lobe, and particularly occipital craniotomies for transtentorial approaches to the retrocallosal area and the pineal region, which require the uplifting of the occipital pole from the oblique falcotentorium transition, can place the opisthocranion as its center. This cranial point is located over the cuneus and over the distal extremity of the calcarine fissure, which should constitute the center of their cortical exposures (*Fig. 18*).

Along the midline, these craniotomies should then expose 1) the POS superior extremity corresponding to the medial extremity of the EOF (EOF/POS) and located underneath the sagittal and lambdoid sutures angle (La/Sa) and 2) the occipital base, which is externally related to the external occipital prominence, or In (9, 59), over the torcula, leaving the opisthocranion, with its underlying cuneus prominence and distal extremity of the calcarine fissure at the center of the cranial and cortical exposures, as already properly illustrated by Seeger (73) and McComb and Apuzzo (47).

Considering the occasional difficulty of palpating the In and estimating the position of the λ, and considering the usual prominence of the opisthocranion, it is interesting to consider that the λ was found to be 2 to 4 cm above the opisthocranion (average distance, 3.00 ± 0.93 cm) and that, according to our previous finding, the In is located between 6 and 8 cm (average distance, 6.80 ± 0.82 cm) inferior to the λ (66) (*Fig. 2*).

Interhemispheric approaches through occipital craniotomies done below the λ usually have the advantage of dealing with fewer bridging veins than in parietal craniotomies (64). It is interesting to note that, along the occipital mesial surface, the opisthocranion, the distal half of the calcarine fissure, the isthmus of the cingulate gyrus, and the splenium are roughly at the same level. Occasional significant cortical visual impairments pertinent to these approaches are particularly related to damage to the borders of the distal half of the calcarine fissure (13).

CONCLUSION

To perform sophisticated cerebral microneurosurgical procedures, precise knowledge and proper identification of the brain sulci and gyri are mandatory in addition to fine microsurgical technique, and, obviously, neurosurgeons cannot be rely only on technological tools. Concurrent with the sulci anatomic variations, which are proportional to a genuine evolutionary sulci hierarchy (71), some of the main sulci extremities and intersections and the sulcal and gyral sites related to prominent cranial points have been shown to have significantly constant neural and cranial topographic relationships. Therefore, they can be considered reliable microneurosurgical key points within an acceptable surgical range.

Together, these sulcal and gyral key points constitute a framework that can help in the understanding of the head and brain tridimensional anatomy and of brain lesions seen in neuroimaging studies, in the positioning of craniotomies, in the sulci intraoperative identification, and in the planning of transsulcal and transgyral procedures. The use of these key points for reaching deep intraventricular and periventricular lesions, and as landmarks to orient the anatomic removal of gyral sectors containing infiltrative tumors through transsulcal approaches is stressed and illustrated.

REFERENCES

1. Apuzzo MJ, Amar AP: The transcallosal interforniceal approach, in Apuzzo MJ (ed): *Surgery of the Third Ventricle.* Baltimore, Williams and Wilkins, 1988, ed 2, pp 421–452.
2. Berger MS, Cohen WA, Ojemann GA: Correlation of motor cortex brain mapping data with magnetic resonance imaging. **J Neurosurg** 72:383–387, 1990.
3. Bischoff TW: Die Grosshirnwindungen des Menschen, Munich, 1868 apud Broca P: Sur la topographie crânie-cerébrale ou sur les rapports anatomiques du crâne et du cerveau. **Rev d'Anthrop** 5:193–248, 1876.
4. Black KL, Pikul BK: Gliomas: Past, present and future. **Clin Neurosurg** 45:160–163, 1997.
5. Black PM, Moriarty T, Alexander E 3rd, Stieg P, Woodard EJ, Gleason PL, Martin CH, Kikinis R, Scwartz RB, Jolesz FA: Development and implementation of intraoperative MRI and its neurosurgical applications. **Neurosurgery** 41:831–842, 1997.
6. Bogen JE: Physiological consequences of complete or partial commissural section, in Apuzzo MJ (ed): *Surgery of the Third Ventricle.* Baltimore, Williams & Wilkins, 1988, ed 2, pp 167–187.
7. Boiling W, Olivier A, Bittar RG, Reutens D: Localization of hand motor activation in Broca's plis de passage moyen. **J Neurosurg** 91:903–910, 1999.
8. Brannen JH, Badie B, Moritz DH, Quigley M, Meyerand ME, Haughton VM: Reliability of functional MR imaging with word-generation tasks for mapping Broca's area. **AJNR Am J Neuroradiol** 22:1711–1718, 2001.
9. Broca P: Diagnostic d'un abcés situé au niveau de la région du langage; trépanation de cet abcès. **Rev d'Anthrop** 5:244–248, 1876.
10. Broca P: Instructions crâniologiques et crâniométriques de la Sociètè d'Anthropologie. Paris, G. Masson, 1875.
11. Broca P: Sur la topographie crânie-cerébrale ou sur les rapports anatomiques du crâne et du cerveau. **Rev d'Anthrop** 5:193–248, 1876.
12. Broca P: Sur les rapports anatomiques des divers points de la surface du crâne et des diverses parties des hémisfères cérébraux. **Bull Soc d'Anth** 2:340, 1861.
13. Brodal A: *Neurological Anatomy in Relation to Clinical Medicine.* New York, Oxford University Press, 1981, ed 3.
14. Carpenter MB: *Human Neuroanatomy.* Baltimore, Williams & Wilkins, 1976, ed 7 , p 547.
15. Chin LS, Levy ML, Apuzzo MJ: Principles of stereotatic neurosurgery, in Youmans JR: *Neurological Surgery.* ed 4, Philadelphia, WB Saunders, 1999, pp 767–785.
16. Constantini S, Pomeranz S, Gomori JM: CT localization of brain tumor. **J Neurosurg** 67:787–788, 1987 (letter).
17. Doran M, Hajnal JV, van Bruggen N, King MD, Young IR, Bydder GM: Normal and abnormal white matter tracts shown by MR imaging using directional diffusion weighted sequences. **J Comput Assist Tomogr** 14: 865–873, 1990.
18. Dorward NL, Alberti O, Palmer JD, Kitchen ND, Thomas DT: Accuracy of true frameless stereotaxy: In vivo measurement and laboratory phantom studies. **J Neurosurg** 90:160–168, 1999.
19. Duvernoy HM: *The Human Brain.* Vienna, Springer, 1991.
20. Ebeling U, Eisner W, Gutbrod K, Ilmberger I, Schmid UD, Reulen HJ: Intraoperative speech mapping during resection of tumors in the posterior dominant temporal lobe. **J Neurol** 369:104, 1992.
21. Ebeling U, Reulen HJ: Neurosurgical topography of the optic radiation in the temporal lobe. **Acta Neurochir (Wien)** 92:26–36, 1988.
22. Ebeling U, Rikli D, Huber P, Reulen HJ: The coronal suture, a useful landmark in neurosurgery? Craniocerebral topography between bony landmarks on the skull and the brain. **Acta Neurochir (Wien)** 89:130–134, 1987.
23. Ebeling U, Schmid UD, Ying Z, Reulen HJ: Safe surgery of lesions near the motor cortex using intra-operative mapping techniques: A report on 50 patients. **Acta Neurochir (Wien)** 119:23–28, 1992.
24. Ebeling U, Steinmetz H: Anatomy of the parietal lobe: Mapping the individual pattern. **Acta Neurochir (Wien)** 136:8–11, 1995.
25. Ebeling U, Steinmetz H, Huang Y, Kahn T: Topography and identification of the inferior precentral sulcus in MR imaging. **AJNR Am J Neuroradiol** 10:101–107, 1989.
26. Ehni G, Ehni BL: Considerations in transforaminal entry, in Apuzzo MJ (ed): *Surgery of the Third Ventricle.* Baltimore, Williams & Wilkins, 1988, ed 2, pp 391–420.
27. Fernandez YB, Borges G, Ramina R, Carelli EF: Double-checked preoperative localization of brain lesions. **Arq Neuropsiquiatr** 61:552–554, 2003.
28. Finger S: *Origins of Neuroscience.* New York, Oxford University Press, 1994.

29. Fitzgerald DB, Cosgrove GR, Ronner S, Jiang H, Buchbinder BR, Belliveau JW, Rosen BR, Benson RR: Location of language in the cortex: A comparison between functional MR imaging and electrocortical stimulation. **AJNR Am J Neuroradiol** 18:152–139, 1997.
30. Gusmão S, Silveira RL, Cabral G: Broca and the birth of modern neurosurgery [in Portuguese]. **Arq Neuropsiquiatr** 58:1149–1152, 2000.
31. Hansebout RR: Surgery of epilepsy, current technique of cortical resection, in Schmidek HH, Sweet WH (eds): *Operative Neurosurgical Techniques,* New York, Grune and Stratton, 1982, pp 963–979.
32. Harkey HL, Al-Mefty O, Haines DE, Smith RR: The surgical anatomy of the cerebral sulci. **Neurosurgery** 24:651–654, 1989.
33. Hinck VC, Clifton GL: A precise technique for craniotomy localization using computerized tomography. **J Neurosurg** 54:416–418, 1981.
34. Horsley V: On the topographical relations of the cranium and the surface of the cerebrum, in Cunningham CJ (ed): *Contribution to the Surface Anatomy of the Cerebral Hemispheres.* Dublin, Academy House, 1892, pp 306–355.
35. Hugher TS, Abou-Khalil B, Lavin PJM, Fakhoury T, Blumenkopf B, Donahue SP: Visual field defects after temporal lobe resection: A prospective quantitative analysis. **Neurology** 53:167–172, 1999.
36. Kamada K, Houkin K, Iwasaki Y, Takeuchi F, Kuriki S, Mitsumori K, Sawamura Y: Rapid identification of the primary motor area by using magnetic resonance axonography. **J Neurosurg** 97:558–567, 2002.
37. King JS, Walker J: Precise preoperative localization of intracranial mass lesions. **Neurosurgery** 6:160–163, 1980.
38. Kocher ET: *Chirurgishe Operationslehre.* Iena, Gustav Fischer, 1907, ed 5.
39. Krause F: *Chirurgie du Cerveau et de la Moelle Epiniere.* Paris, Societé D'Editions Scientifiques et Medicales, 1912.
40. Krings T, Reinges MT, Thiex R, Gilsbach JM, Thron A: Functional and diffusion-weighted magnetic resonance images of space-occupying lesions affecting the motor system: Imaging the motor cortex and pyramidal tracts. **J Neurosurg** 95:816–824, 2001.
41. Krol G, Galicich J, Arbit E, Sze G, Amster J: Preoperative localization of intracranial lesions on MR. **AJNR Am J Neuroradiol** 9:513–516, 1988.
42. Krönlein RU: *Topographie Cranio Cérébrale.* V. Bruns' Beiträge zur Keinishen Chirurgie, 1898, p 364.
43. Lang J: *Mikroanatomischer Kurs für junge Neurochirurgen.* Anatomisches Institut der Universität Würzburg, 1985.
44. Lavyne MH, Patterson RH: The subchoroidal trans-velum interpositum approach, in Apuzzo MJ (ed): *Surgery of the Third Ventricle.* Baltimore, Williams & Wilkins, 1988, ed 2, pp 453–470.
45. Lobel E, Kahane P, Leonards U, Grosbras M-H, Lehéricy S, Le Hihan D, Berthoz A: Localization of human frontal eye fields: Anatomical and functional findings of functional magnetic resonance imaging and intracerebral electrical stimulation. **J Neurosurg** 95:804–815, 2001.
46. McComb JG: Methods of cerebrospinal fluid diversion, in Apuzzo MJ (ed): *Surgery of the Third Ventricle.* Baltimore, Williams & Wilkins, 1988, ed 2, pp 607–634.
47. McComb JG, Apuzzo MJ: Posterior intrahemispheric retrocallosal and transcallosal approaches, in Apuzzo MJ (ed): *Surgery of the Third Ventricle.* Baltimore, Williams & Wilkins, 1988, ed 2, pp 611–640.
48. Moore DS: *Statistics, Concepts and Controversies.* 3rd ed. New York, WH Freeman, 1991.
49. Naidich TP, Brightbill TC: Systems for localizing fronto-parietal gyri and sulci on axial CT and MRI. **Int J Neuroradiol** 2:313–338, 1996.
50. Naidich TP, Valavanis AG, Kubik S: Anatomic relationships along the low-middle convexity: Part I—Normal specimen and magnetic resonance imaging. **Neurosurgery** 36:517–532, 1995.
51. Naidich TP, Valavanis AG, Kubik S, Taber KH, Yaşargil MG: Anatomic relationships along the low-middle convexity: Part II—Lesion localization. **Int J Neuroradiol** 3:393–409, 1997.
52. O'Leary DH, Lavyne MH: Localization of vertex lesions seen on CT scan. **J Neurosurg** 49:71–74, 1978.
53. Ojemann G, Ojemann J, Lettich E, Berger M: Cortical language localization in left dominant hemisphere: An electrical stimulation mapping investigation in 117 patients. **J Neurosurg** 71:316–326, 1989.
54. Ono M, Kubik S, Abernathey CD: *Atlas of Cerebral Sulci.* Stuttgart, Thieme, 1990.
55. Passet J: Über einige Unterschiede des GroBhirns nach dem Geschlecht. **Archiv für Anthropologie (Braunschweig)** 14:89–141, 1882.
56. Penfield W, Rasmussen T: *The Cerebral Cortex of Man.* New York, MacMillan, 1952.
57. Penfield WG, Boldrey E: Somatic motor and sensory representation in the cerebral cortex of man as studied by electrical stimulation. **Brain** 60:389–443, 1937.
58. Penning L: CT localization of a convexity brain tumor on the scalp. **J Neurosurg** 66:474–476, 1987.
59. Pernkoff E: *Atlas of Topographical and Applied Human Anatomy.* Baltimore, Urban & Schwarzenberg, 1980.
60. Pia HW: Microsurgery of gliomas. **Acta Neurochirurgica** 80:1–11, 1986.
61. Pierpaoli C, Jezzard P, Basser PJ, Barnett A, Di Chiro G: Diffusion tensor MR imaging of the human brain. **Radiology** 201:637–648, 1996.
62. Quiñones-Hinojosa A, Ojemann SG, Sanai N, Dillon WP, Berger MS: Preoperative correlation of intraoperative cortical mapping with magnetic resonance imaging landmarks to predict localization of the Broca area. **J Neurosurg** 99:311–318, 2003.
63. Rasmussen TB, Milner B: Clinical and surgical studies of the cerebral speech areas in man, in Zulch KJ, Creutzfeldt O, Galbraith GC (eds): *Cerebral Localization.* New York, Springer-Verlag, 1975, pp 238–257.
64. Rhoton AL Jr: Cranial anatomy and surgical approaches. **Neurosurgery** 53:1–746, 2003.
65. Rhoton AL Jr: General and micro-operative techniques, in Youmans JR (ed): *Neurological Surgery.* Philadelphia, WB Saunders, 1999, ed 4, pp 724–766.
66. Ribas GC: Study of the anatomic relationships of the lambdoid, occipitomastoid and parietomastoid sutures with the transverse and sigmoid sinuses, and of regional burr hole sites [in Portuguese]. São Paulo, Universidade de São Paulo, 1991 (dissertation).
67. Ribas GC, Bento RF, Rodrigues AJ Jr: Anaglyphic three-dimensional stereoscopic printing: revival of an old method for anatomical and surgical teaching and reporting. Tecnhical note. **J Neurosurg** 95:1057–1066, 2001.
68. Roberts DW, Hartov A, Kennedy FE, Miga MI, Aulsen KD: Intraoperative brain shift and deformation: A quantitative analysis of cortical displacement in 28 cases. **Neurosurgery** 43:749–760, 1998.
69. Rowland LP, Mettler FA: Relation between the coronal suture and cerebrum. **J Comp Neurol** 89:21–40, 1948.
70. Rutten GM, Ramsey NF, Van Rijen PC, Noordmans HJ, Van Veelen CM: Development of a functional magnetic resonance imaging protocol for intraoperative localization of critical temporoparietal language areas. **Ann Neurol** 51:350–360, 2002.
71. Sarnat HB, Netsky MG: *Evolution of the Nervous System.* New York, Oxford University Press, 1981, ed 2.
72. Schiffbauer H, Berger MS, Ferrari P, Freudenstein D, Rowley HA, Roberts TP: Preoperative magnetic source imaging for brain tumor surgery: A quantitative comparison with intraoperative sensory and motor mapping. **J Neurosurg** 97:1333–1342, 2002.
73. Seeger W: *Atlas of Topographical Anatomy of the Brain and Surrounding Structures.* Vienna, Springer, 1978.
74. Seeger W: *Microsurgery of Intracranial Tumors.* Vienna, Springer-Verlag, 1995.
75. Seeger W: *Microsurgery of the Brain, Anatomical and Technical Principles.* Vienna, Springer, 1980.
76. Shucart W: The anterior transcallosal and transcortical approaches, in Apuzzo MJ (ed): *Surgery of the Third Ventricle.* Baltimore, Williams & Wilkins, 1988, ed 2, pp 369–390.
77. Siegel S, Castellan NJ: *Nonparametric Statistics for the Behavioral Sciences.* New York, McGraw-Hill, 1988, ed 2.
78. Simos PG, Papanicolaou AC, Breier JI, Wheless JW, Constatinou JC, Gormley WB, Maggio WW: Localization of language-specific cortex by using magnetic source imaging and electrical stimulation mapping. **J Neurosurg** 91:787–796, 1999.
79. Squire LR, Bloom FE, McConnell SK, Roberts JL, Spitzer NC, Zigmond MJ: *Fundamental Neuroscience.* Amsterdam, Academic Press, 2003, ed 2.
80. Steinmetz H, Ebeling U, Huang YX, Kahn T: Sulcus topography of the parietal opercular region: An anatomic and MR study. **Brain Lang** 38:515–533, 1990.
81. Sure U, Alberti O, Petermeyer M, Becker R, Bertalanffy H: Advanced image guided skull base surgery. **Surg Neurol** 53:563–572, 2000.
82. Tamraz JC, Comair YG: *Atlas of Regional Anatomy of the Brain using MRI.* Berlin, Springer, 2000.

83. Taylor EH, Haugton WS: Some recent researches on the topography of the convolutions and fissures of the brain. **Trans R Acad (Ireland)** 18:511–519, 1900.
84. Testut L, Jacob O: *Text of Topographic Anatomy* [in Portuguese]. Barcelona, Salvat, 1932, ed 5.
85. Türe U, Yaşargil DH, Al-Mefty O, Yaşargil MG: Topographic anatomy of the insular region. **J Neurosurg** 90:730–733, 1999.
86. Uematsu S, Lesser R, Fisher RS, Gordon B, Hara K, Krauss GL, Vining EP, Webber RW: Motor and sensory cortex in humans: Topography studied with chronic subdural stimulation. **Neurosurgery** 31:59–72, 1992.
87. Unsgaard G, Ommedal S, Muller T, Gronningsaeter A, Nagethus Hermes TA: Neuronavigation by intraoperative three-dimensional ultrasound: Initial experience during brain tumor resection. **Neurosurgery** 50:804–812, 2002.
88. Vogt O, Vogt C: Ergebnisse unserer Hirnförshung, in Penfield W, Erickson TC (eds): *Epilepsy and Cerebral Localization*. Springfield, Charles C. Thomas, 1941, pp 277–462..
89. von Economo C, Koskinas GN: *Die Cytoarchitektonik der Hirnrinde des Erwachsenen Menschen. Textband und Atlas.* Vienna, Springer, 1925.
90. Watanabe E, Watanabe T, Manaka S, Mayanagi Y, Takakura K: Three-dimensional digitizer (neuronavigator): New equipment for computed tomography-guided stereotatic surgery. **Surg Neurol** 6:543–547, 1987.
91. Wen HT, Rhoton AL Jr, de Oliveira EP, Cardoso AC, Tedeschi H, Baccanelli M, Marino R Jr: Microsurgical anatomy of the temporal lobe: Part I: Mesial temporal lobe anatomy and its vascular relationships and applied to amygdalohippocampectomy. **Neurosurgery** 45:549–592, 1999.
92. Wirtz CR, Bonsanto MM, Knauth M, Tronnier VM, Albert FK, Staubert A, Kunze S: Intraoperative MRI to update interactive navigation in neurosurgey: Method and preliminary experience. **Comput Aided Surg** 2:172–179, 1997.
93. Witwer BP, Moftakhar R, Hasan KM, Deshmukh P, Haughton V, Field A, Arfanakis K, Noyes J, Moritz CH, Meyerand ME, Rowley HA, Alexander AL, Badie B: Diffusion-tensor imaging of white matter tracts in patients with cerebral neoplasm. **J Neurosurg** 97:568–575, 2002.
94. Yaşargil MG: Legacy of microneurosurgery: Memoirs, lessons, and axioms. **Neurosurgery** 45:1025–1091, 1999.
95. Yaşargil MG: *Microneurosurgery.* Stuttgart, Georg Thieme, 1984, vol. I.
96. Yaşargil MG: *Microneurosurgery.* Stuttgart, Georg Thieme, 1994, vol. IVa.
97. Yaşargil MG: *Microneurosurgery.* Stuttgart, Georg Thieme, 1996, vol. IVb.
98. Yaşargil MG, Abdulrauf SI: Image-guided transsylvian, transinsular approach for insular cavernous angiomas. **Neurosurgery** 2003; 53:1299–1305 (comment).
99. Yaşargil MG, Cravens GF, Roth P: Surgical approaches to "inaccessible" brain tumors. **Clin Neurosurg** 34:42–110, 1988.
100. Yaşargil MG, Fox JL, Ray MW: The operative approach to aneurysms of the anterior communicating artery, in Krayenbül H (ed): *Advances and Technical Standards in Neurosurgery.* Vienna, Springer-Verlag, 1975, pp 114–170.
101. Yaşargil MG, Kasdaglis K, Jain KK, Weber HP: Anatomical observations of the subarachnoid cisterns of the brain during surgery. **J Neurosurg** 44:298–302, 1976.
102. Yaşargil MG, Krisht AF, Türe U, Al-Mefty O, Yaşargil DC: Microsurgery of insular gliomas: Part I: Surgical anatomy of the sylvian cistern. **Contemp Neurosurg** 24:1–8, 2002.
103. Yaşargil MG, Krisht AF, Türe U, Al-Mefty O, Yaşargil DC: Microsurgery of insular gliomas: Part II: Opening of the sylvian fissure. **Contemp Neurosurg** 24:1–5, 2002.
104. Yaşargil MG, Türe U, Roth P: A combined approach, in Apuzzo MJ (ed): *Surgery of the Third Ventricle.* Baltimore, Williams and Wilkins, 1988, ed 2, pp 541–552.
105. Yousry TA, Schmid UD, Jassoy AG, Schmidt D, Eisner WE, Reulen HJ, Reiser MF, Lissner J: Topography of the cortical motor hand area: Prospective study with functional MR imaging and direct motor mapping at surgery. **Radiology** 195:23–29, 1995.

COMMENTS

Ribas et al. present an excellent study on the anatomy of cerebral sulci and their correlation with surgically important cranial points. They found consistent cranial-cerebral relationships that can be used as landmarks for the placement of craniotomies, for the transsulcal approaches to deep-seated lesions, and to orient the removal of infiltrative tumors. The article is illustrated with practical three-dimensional (3-D) images that clarify the relationships between structures in different layers.

The concept of see-through x-ray-type knowledge of the supratentorial area is of paramount importance in neurosurgery. The location of selected deep structures in relation to cranial and superficial cerebral landmarks has been examined elsewhere (1). In this article, the authors validated, by means of statistical analyses, the utility of some well-known cranial and cortical/sulcal landmarks, reintroduced useful craniometric points such as the stephanion or the euryon, and created new cranial points related to important cortical/sulcal points. We had the opportunity to test in the laboratory the 10 sulcal key points studied by Ribas et al., and we found, as the authors described, the sulcal points were identified within an interval not bigger than 2 cm in relation to their correspondent cranial points. Because the validation of the sulcal key points come from an anatomical study, it would have been very interesting to know about the authors' experience regarding modification of those cranial-cerebral relationships caused by expansive tumors and their surrounding edema.

We agree with the authors that precise knowledge of microneurosurgical anatomy is the basis to navigate safely around and through the cerebrum. Technological tools can provide important assistance, but they will never replace such knowledge. In addition, the combination of 3-D anatomical expertise with intraoperative cortical and subcortical stimulation, when indicated, is the best ally in performing successful glioma surgery.

This article is highly recommended for residents and all neurosurgeons. It will become an important reference on topographical neuroanatomy.

Albert L. Rhoton, Jr.
Juan Carlos Fernandez-Miranda
Gainesville, Florida

---

1. Rhoton AL Jr: The cerebrum. **Neurosurgery** 51 [Suppl 1]:S1-S51, 2002.

The authors review the topographic anatomy of the cranium, stressing the relationships that the main cranial key points have with the underlying cerebral superficial anatomy and with the main sulci in particular. These relationships are of growing importance, as the concept of minivasiveness is spreading throughout the neurosurgical community. Mininvasive neurosurgery is often an abused term whose use should be circumscribed to those procedure that are planned to minimize brain damage, not only superficial layers damage. The amplitude of the superficial layers opening should be decided only after having planned the kind of cerebral exposure that is required to get to the targeted pathology and not vice versa. This means that surgical planning should start with the precise identification on the neuroradiological images available in the navigation system of the sulcus that can provide access to the lesion. The authors are providing the neurosurgical community with a formidable mean to interact with the working station and double check the intraoperative information that the system of navigation is giving to the operating surgeon. In addition, their study confirms what Yaşargil taught to all the neurosurgeons (i.e., that sulci and cisterns are to be followed to transform a deep lesion into a superficial one). If the sulcus is widely and sharply opened under strong magnification, any damage to the pial surface and deep vessels can be avoided in most patients, and only this kind

of technique should be called minivasive. The diameter of craniotomy is, in our experience, calibrated on the preplanned length of sulcal opening that is related to the depth of the targeted lesion. The deeper the lesion, the longer the arachnoidal opening must be in order to avoid undue traction on the pial surface of the sulcal lips. This allows for minimizing and generally avoiding the use of retractors, keeping in mind that gravity should be the favorite neurosurgical retractor. We plan the skin incision last and very often a linear incision is sufficient. This work can be done on the 3-D model of the neuronavigation system (or on the two-dimensional radiological images, if image guidance is unavailable) prior to working on the patient's skin. The authors studied cranial points that constitute the fundamental landmarks for transferring the work that done in the workstation onto the patient's skin prior to registration. In our department, residents must draw the incision before registration and then double check it by the use of image guidance. I am sure that the number of times they will have to change their initial drawing will dramatically decrease after reading this article.

The authors have provided an instrument that can greatly help in our daily surgical practice.

Giovanni Broggi
Paolo Ferroli
Milan, Italy

The authors have undertaken an exhaustive study of the key sulcal and gyral anatomical landmarks. Although there have been many previous studies of cortical mapping and detailed microneuroanatomical publications, there has been little published on anatomical cranial-cerebral correlations. This study details both previous data and adds significant new information.

Although modern neuronavigation systems have largely replaced the time-honored cerebral-cranial localization methods used by neurosurgeons, I would agree with the authors that it is essential when training neurosurgeons, particularly those who have become reliant on neuronavigation methods, to have a strong understanding of basic neurosurgical anatomy, which includes knowledge of cranial-cerebral relationships that are fundamental to neurosurgery. Such knowledge considerably enhances the 3-D understanding of the complex cranial-cerebral anatomy. It is essential not to become over-reliant on technology, as we have all experienced perioperative failures of navigation systems, and in such circumstances, have needed to revert to the use of basic neuroanatomy. In addition, there are many countries where neuronavigation systems are not readily available, and of course, such data as presented here is invaluable in this situation.

It is necessary to interpret these anatomical studies in a clinical situation where brain shift due to tumors and other pathologies could result in a movement of the sulcal key points. However, this does not diminish the importance of this basic neuroanatomical information.

The authors are to be commended for their excellent study, the details of which should be understood by all practicing neurosurgeons.

Andrew H. Kaye
Parkville, Australia

Ribas et al. provide a *tour de force* in correlating surface cortical landmarks to craniometric points. The goal of their study is not to return us to the age of Broca, but to reinforce the familiarization that trainees in neurosurgery must have in order to operate on the brain. Training must emphasize the incorporation of the 3-D anatomic system within the minds of residents and fellows to navigate through the brain.

Although navigation systems are a technological advance, we cannot train our junior colleagues to rely solely on these systems to help them find their way through the brain and to accomplish operative goals. Navigation systems are a tool. However, if a fundamentally greater understanding of anatomy is not acquired, surgery on the brain becomes analogous to doing math on a calculator without insight into the actual mathematical operations. In many parts of the world that lack expensive technology for navigation or imaging, reliance on the self-incorporated 3-D anatomic system correlated with a detailed clinical examination is the only means by which surgery can be performed confidently. Understanding anatomical fundamentals affects our abilities to conduct neuroanatomical research and to assess whether or not there are better ways to approach our targets.

Readers of this study may find themselves hearkening to the methods of brain operation navigation originally published by Broca (1, 2) in 1876 and elaborated by Poirier (4), Reid and Mullingan (5), Taylor and Houghton (8), and Rhoton (7). These procedures have guided craniotomies for more than 100 years. Until computed tomography was applied to the development of image-guided surgical systems, these procedures were the only means to guide placement of incisions (6). In fact, for most craniotomies, these methods held sway over the stereotactic systems for decades, even when stereotactic systems would have improved accuracy, especially to deep structures. The primary impact of image-guided navigation systems has been to reveal pathologies that distort the brain.

In 1892, Horsley (3) commented that a craniotopographic system that could account for brain shift would be a remarkable advance for guiding a craniotomy. Neurosurgery residents, like Broca and his student Champonniere, should develop a mental image of cortical surface locations and even deeper structures that correlate to head positions. Planning craniotomies in this manner serves as an inner check on the navigation system, provides a more satisfying educational outcome for each case, and may improve surgical outcomes for patients.

Mark C. Preul
Robert F. Spetzler
Phoenix, Arizona

1. Broca P: Diagnosis of an abscess situated at the level of the region of language: Trephination for this abscess [in French]. **Rev d'Anthrop** 5:244–248, 1876.
2. Broca P: On Cranial-Cerebral Topography, or on Anatomic Reports of the Cranium and Brain [in French]. **Rev d' Anthrop** 5:193–248, 1876.
3. Horsley V: On the topographical relations of the cranium and surface of the cerebrum, in Cunningham DJ (ed): *Contribution to the Surface Anatomy of the Cerebral Hemispheres.* Dublin, Academy House, 1892, pp 306–355.
4. Poirier PJ: *Topographie Cranio-Encéphalique. Num BNF de l'éd.* Paris, Lecrosnier et Babé, 1891.
5. Reid RW, Mullingan JH: Communications from the anthropometric laboratory of the University of Aberdeen. **Journal of the Royal Anthropological Institute of Great Britain and Ireland** 54:287–315, 1924.
6. Reis CV, Crusius M, Deshmukh P, Zabramski JM, Spetzler RF, Preul MC: Comparative study of cranial topographic procedures for determination of central and lateral sulci of the brain: Putting history to the test. Presented at the Annual Meeting of the American Association of Neurological Surgeons, San Francisco, April 26, 2006.
7. Rhoton Al Jr: The cerebrum. **Neurosurgery** 51 [Suppl 4]:S1–S51, 2002.
8. Taylor EH, Haughton WS: Some recent researches on the topography of the convolutions and fissures of the brain. **Trans R Acad Med Ireland** 18:511–522, 1900.